



Universiteit
Leiden
The Netherlands

Design, synthesis, characterization and biological studies of ruthenium and gold compounds with anticancer properties

Garza-Ortiz, A.

Citation

Garza-Ortiz, A. (2008, November 25). *Design, synthesis, characterization and biological studies of ruthenium and gold compounds with anticancer properties*. Retrieved from <https://hdl.handle.net/1887/13280>

Version: Corrected Publisher's Version

License: [Licence agreement concerning inclusion of doctoral thesis in the Institutional Repository of the University of Leiden](#)

Downloaded from: <https://hdl.handle.net/1887/13280>

Note: To cite this publication please use the final published version (if applicable).

CHAPTER 4

Synthesis of New Bis(arylimino)pyridine-Ru(III) Compounds.
 Characterization and Elucidation of the Paramagnetic Structure
 by means of Nuclear Magnetic Resonance.
 DNA-model Base Studies and Cytotoxic Properties*

Abstract

In search of new metal-based anticancer compounds, Ru(III/II) complexes have deserved special attention not only because of their good antitumour activity in screening studies, but also because of their cancer-cell specific targeting properties.

The need of more biological and chemical evidence in the reactivity of Ru(III/II) systems has encouraged, the synthetic, spectroscopic, structural and biological studies of two novel bis(arylimino)pyridine Ru(III) chloride compounds containing the ligands, 2,6-bis(2,4,6-trimethylphenyliminomethyl)pyridine and 2,6-bis(2,6-diisopropylphenyliminomethyl)pyridine is described in this chapter. The bis(arylimino)pyridine ligands were synthesized by condensation of 2,6-pyridinedicarboxaldehyde with 2,4,6-trimethylaniline or 2,6-diisopropylaniline and further characterized in the solid state through monocystal X-ray diffraction analysis and other standard characterization techniques. The Ru(III) compounds, with general formula $[\text{RuCl}_3(\text{L})] \cdot x(\text{H}_2\text{O})$, where $\text{L}=\text{L}1=2,6\text{-bis}(2,4,6\text{-trimethylphenyl-iminomethyl)pyridine}$, $\text{L}2=2,6\text{-bis}(2,6\text{-isopropylphenylimino methyl)pyridine}$ and $x=0$ or 1 , named RuL1 and RuL2 respectively, were structurally determined on the basis of analytical and spectroscopic (IR, UV-Vis, ESI-MS, EPR) studies. A complete assignment of the ^1H NMR resonances of the two paramagnetic compounds was made in deuterated dmf by one- and two-dimensional techniques. These new compounds are intended to constitute a series of new anticancer Ru(III) and Ru(II) compounds with improved cytostatic properties; likely to be modified in a desirable manner due to the relatively facile ligand modification of the bis(imino)pyridines and their molecular architecture.

Although the ligands by themselves are moderately cytotoxic in selected cell lines (EVSA-T and MCF-7), the anticancer activity of the $[\text{Ru}(\text{L})\text{Cl}_3] \cdot x\text{H}_2\text{O}$ compounds is significant for a broad range of cancer cell-lines tested *in vitro* (IC_{50} values = $4 \sim 17 \mu\text{M}$). Finally, reaction of RuL1 with the DNA model base, 9-ethylguanine (9EtGua) was found to produce in a redox reaction, the species *trans*- $[\text{Ru}(\text{II})(\text{L}1)(9\text{EtGua})_2(\text{H}_2\text{O})](\text{ClO}_4)_2$ (abbreviated as RuL1-2(9EtGua)) which was fully characterized by conventional methods in solution and also in the solid state, by X-ray crystallography. The structure comprises the as yet unknown *trans*-bis(purine)-Ru(II) unit.

"We especially need imagination in science. It is not all mathematics, nor all logic, but it is somewhat beauty and poetry"

Maria Montessori, physician, educator, philosopher (1870-1952)

* Some of the results presented in this chapter have been published Garza-Ortiz, A.; Maheswari, P. U.; Siedler, M.; Spiek, A. L. and Reedijk, J.. *Inorg. Chem.* 47 (2008) 6964-6973.

4.1 Introduction

After the serendipitous discovery of cisplatin [1], the most successful platinum-based anticancer compound, attention to other anticancer metal-based compounds has been directed [2-7] in a search for less toxic and more effective drugs.

Among all the metals used in the synthesis of potential anticancer drugs, a wide range of ruthenium compounds have been described in the literature, some of them with outstanding anticancer activity [8-15] and two of them, i.e. NAMI-A and KP1019, are currently involved in clinical trials [16-18].

It is known that ruthenium compounds are well suited for medical applications due to the fact of having convenient rates of ligand exchange [19], a range of accessible oxidation states and the ability of ruthenium to mimic iron in binding to certain biological molecules [8, 10, 17]. Under aqueous conditions, three predominant oxidation states are known for ruthenium, i.e. Ru(II), Ru(III) and Ru(IV), all of them mostly presenting an octahedral configuration. This octahedral geometry appears to be partially responsible for the differences observed in the mechanism of action compared with cisplatin. The hypoxic environment of many tumours may favour the reduction of Ru(III) compounds (which are relatively slow to bind to most biological substrates) to Ru(II) species, which bind more rapidly [10]. Among ruthenium compounds studied for anticancer application, the group of ruthenium compounds with pyridyl-based ligands is of special interest, due to a combination of easily constructed rigid chiral structures and useful photophysical properties. They mostly have been studied because when chiral, they are capable of enantioselective recognition of DNA and they display cleavage properties as well [20-37]. As the majority of these compounds contain bidentate ligands with functional auxiliary ligands, research on Ru(III)/Ru(II) complexes with more rigid, tridentate ligands and additional chloride ligands is a new challenge.

In fact, considerable cytotoxic activity of compounds with structural formulas: $[\text{Ru}(\text{bpy})(\text{tpy})\text{Cl}]\text{Cl}$ and *mer*- $[\text{Ru}(\text{tpy})\text{Cl}_3]$ (bpy = 2,2'-bipyridyl, tpy = 2,2':6',2''-terpyridine) has been demonstrated in murine and human tumour cell lines [38, 39]. *mer*- $[\text{Ru}(\text{III})\text{Cl}_3(\text{tpy})]$ exhibits a remarkably higher cytotoxicity than the other compounds and even displays the highest [22] and remarkable DNA interstrand cross-linking properties. Unfortunately solubility problems and - even more importantly - difficulties in preparation of terpyridine derivatives have reduced the attention for this system.

During the last decade bis(imino)pyridine ligands (figure 4.1) have attracted significant attention [40-46], due to their easy synthesis, possibility of steric and electronic tuning, and well-documented ability to support a range of catalytically active metal centres (especially for iron and cobalt) and other interesting structural types. In particular their redox activity has been studied intensely and in general the variety of chemistry displayed for this ligand system is remarkable [47].

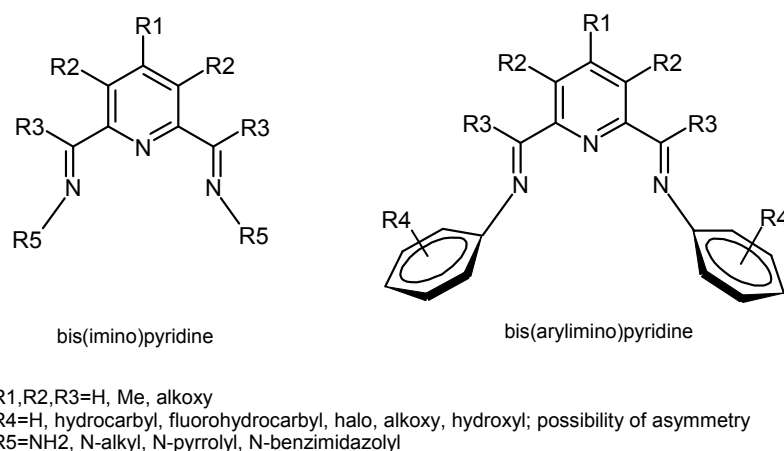


Figure 4.1 Schematic representation of tridentate bis(imino)pyridine and bis(arylimino)pyridine derivatives.

Most probably the origin of the synthesis of this kind of structures resides in the study of the coordination properties of Co(II), Fe(II) and Ni(II) [48]. Among the best known complexing agents for these metals, heterocyclic diamines and triamines (like 2,2'-bipyridyl), α -dioximes (like

dimethylglyoxime) and α -diimines are to be mentioned. Then more elaborated organic systems were designed and synthesized, where the previously mentioned organic functionalities were included at the same time, and among them 2,6-bis(imino)pyridine systems were fully described. They also attracted attention due to their tridentate nature, simple synthetic procedures and close chemical similarities with terpyridine, a less accessible to be chemically modified ligand [49].

Attention to the coordination chemistry of classic tridentate nitrogen donor ligands with transition metal ions was revitalized as a result of the unexpected discovery that these type of compounds are very active olefin polymerization catalysts. In particular, pyridine-2,6-diimine ligands like 2,2':6,2''-terpyridine analogues and their iron and cobalt compounds have shown significant activity [44]. Later on structural modifications in the ligands, in the search of better activity, led to the discovery of bis(imino)pyridine-transition metal complexes (Co and Fe) [50-53] with high catalytic activity and unlike traditional ligands for olefin polymerization, these ligands show a rich chemistry by their own, due mainly to the potentially reactive sites, including the nitrogen carbon centre of the imine moiety and the pyridine ring, capable even of accommodate up to three electrons in their antibonding orbitals [54]. Finally it is important to mention that similar Schiff-base ligands are widespread in the use to mimic biological systems for multiple chemical transformations; bis(arylimino)pyridine-Cu compounds have been extensively studied as models for blue copper proteins [40].

In the present chapter the Ru(III) chemistry with the tridentate ligands 2,6-bis(2,4,6-trimethylphenyliminomethyl)pyridine, 2,6-bis(2,6-diisopropylphenyliminomethyl)pyridine, 2,6-bis(4-methylphenyliminomethyl)pyridine and 2,6-bis(phenyliminomethyl)pyridine (abbreviated L1, L2, L3 and L4 respectively and schematically represented in figure 4.2) was studied. All these Schiff bases can coordinate to Ru(III) via the pyridine nitrogen and the two imine nitrogen donors. The coordinating nitrogen atoms present three in-plane bonding positions, in which only the three meridional positions of an octahedron can be occupied by the donor nitrogen atoms. In this respect these ligands behave like 2,2':6,2''-terpyridine. A study of the literature reveals that little ruthenium chemistry on this type has been carried out.

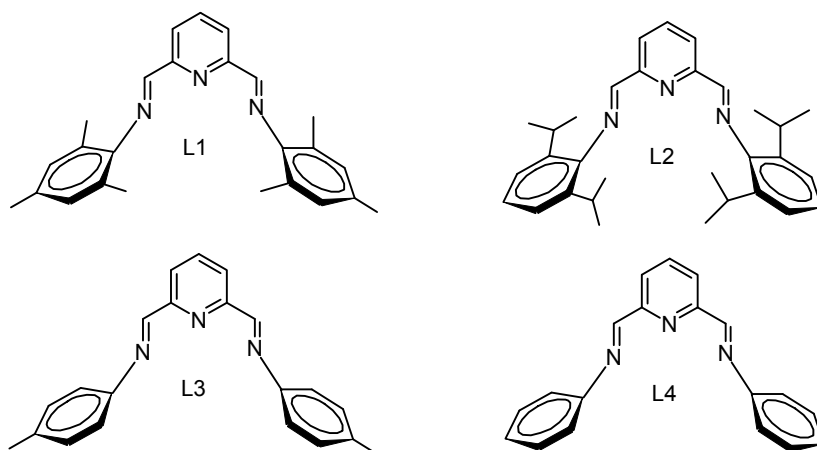


Figure 4.2 Schematic representation of tridentate bis(arylimino)pyridine derivatives used in the synthesis of the Ru(III) compounds described in this chapter. 2,6-bis(2,4,6-trimethylphenyliminomethyl)pyridine (L1), 2,6-bis(2,6-diisopropylphenyliminomethyl)pyridine (L2), 2,6-bis(4-methylphenyliminomethyl)pyridine (L3) and 2,6-bis(phenyliminomethyl)pyridine (L4).

The main goal of this research project is the search for new anticancer-active systems based on ruthenium(III) and a prototype series of Ru compounds, using a versatile tridentate bis(imino)pyridine-type of molecule as chelating ligand have been synthesized and characterized. The successfully isolated compounds, fully characterized by elemental analysis, IR, ^1H NMR, UV-Vis, EPR and ESI mass spectroscopy as octahedral compounds, keep three coordination sites occupied by labile chloride ligands (figure 4.3).

^1H NMR characterization in Ru(III) ions is hampered due to the presence of the unpaired electron in the t_{2g} orbital of the low-spin d^5 ion. The resulting paramagnetism induces hyperfine shifts of the ^1H NMR signals and shortening of nuclear longitudinal (T_1) and transverse (T_2) relaxation times, which hinders the application of standard ^1H NMR techniques and assignment procedures for diamagnetic molecules. Despite this limitation, a complete assignment of

resonance peaks in the spectra was achieved through comparison with related systems, integration values and shifts, thereby providing more evidence in the characterization of these paramagnetic compounds.

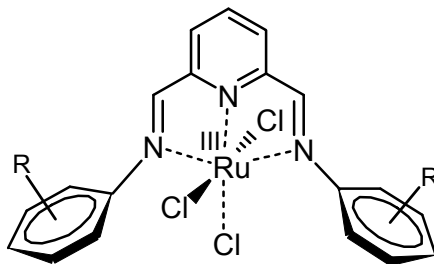


Figure 4.3 General schematic representation of Ru(III)-bis(arylimino)pyridine derivatives described in this chapter.

The major advantage of this family of Ru compounds is that the bis(imino)pyridine ligands can be chemically modified to tune its solubility, its cytotoxicity and also the pharmacokinetics and pharmacodynamics in the human body.

Even though the mechanism of action of cytotoxic Ru(III) compounds has not been completely elucidated, a direct interaction with DNA is a likely possibility, among other mechanisms. With respect to this prototype family of Ru compound, the chemical interaction between it and the DNA model base, 9-ethylguanine (9EtGua), was studied in solution, but also by X-ray diffraction of the isolated crystals of the adduct formed. This study pursues to shed some light on the chemical interaction of this new family of Ru(III) compounds with DNA.

The promising cytotoxic activity observed for the compounds synthesized encourage further studies and the synthesis of more derivatives that could provide more chemical evidence, useful in the proposal of structure-activity relationships.

4.2 Experimental section

4.2.1 Methods and instrumental techniques

A. X-ray Crystallography. All reflections intensities were measured at 150(2) K using a Nonius KappaCCD diffractometer (rotating anode for L1, L2 and L3 and fine-focus sealed tube for RuL1-2(9EtGua)) equipped with graphite-monochromated Mo $K\alpha$ radiation ($\lambda = 0.71073 \text{ \AA}$) under the program *COLLECT* [55]. The program *PEAKREF* [56] was used to determine the cell dimensions. The two sets of data were integrated using the program *EVALCCD* [57]. The structure of L1, L2 and L3 was solved with the program *SHELXS86* [58] and that of RuL1-2(9EtGua) with the program *DIRDIF99* [59]. All the structures were refined on F^2 with *SHELXL97* [60]. Multi-scan semi-empirical absorption corrections were applied to the sets of data using *SADABS* [61]. For L1, 2026 reflections were unique ($R_{\text{int}} = 0.037$), of which 1637 were observed ($\theta_{\text{max}} = 26^\circ$) with the criterion of $I > 2\sigma(I)$; for L2, 6182 reflections were unique ($R_{\text{int}} = 0.051$), of which 4401 were observed ($\theta_{\text{max}} = 27.5^\circ$) with the criterion of $I > 2\sigma(I)$; for L3, 1576 reflections were unique ($R_{\text{int}} = 0.071$), of which 1051 were observed ($\theta_{\text{max}} = 25.6^\circ$) with the criterion of $I > 2\sigma(I)$; for RuL1-2(9EtGua), 5448 reflections were unique ($R_{\text{int}} = 0.015$), of which 5276 were observed ($\theta_{\text{max}} = 27.5^\circ$) with criterion of $I > 2\sigma(I)$. The *PLATON* software [62] was used for molecular graphics, structure checking and calculations. The H-atoms were placed at calculated positions (except as specified) with isotropic displacement parameters having values 1.2 or 1.5 times U_{eq} of the attached atom. For L1, the H-atoms of the two methyl groups C11 (*ortho* position) and C12 (*para* position) were found to be disordered by a rotation of 60° and were treated using the *AFIX 123* instruction. The occupation factors for the two major components of the disorder refined to 0.73(2) and 0.77(3). For L2, the H-atom of C16 and the two methyl groups C17 and C18 were found to be disordered by a rotation of 18° and were treated using the *AFIX 123* instruction. For RuL1-2(9EtGua), the H-atoms for the atoms O1 and N5 were located from the difference Fourier map and the O–H and N–H bond distances were restrained to be 0.84 and 0.88 \AA (using the *DFIX* instruction). Crystallographic data for L1, L2 and L3 are listed in Appendix A, while crystallographic data for RuL1-2(9EtGua) are listed in tables 4.7 and 4.8.

B. NMR Spectroscopy. ^1H NMR experiments were recorded on a Bruker 300 DPX spectrometer using 5 mm NMR tubes. All spectra were recorded at 294 K, unless otherwise indicated. The temperature was kept constant using a variable temperature unit. The software XWIN-NMR and XWIN-PLOT were used for edition of the NMR spectra. Tetramethylsilane (TMS) or the deuterated solvent residual peaks were used for calibration. In addition, 2D ^1H COSY spectra were recorded to confirm the proton assignments from 1D measurements.

C. C,H,N Analysis. Elemental analyses were performed with a Perkin Elmer series II CHNS/O 2400 Analyzer.

D. Mass Spectroscopy. Electrospray mass spectra were recorded on a Finnigan TSQ-quantum instrument using an electrospray ionization technique (ESI-MS). The eluent used was the mixture acetonitrile:water 80:20.

E. Other methods. The UV-Visible (UV-Vis) spectra were recorded using a Varian CARY 50 UV/VIS spectrophotometer operating at RT. The electronic spectra were recorded in freshly prepared solutions of each compound. The IR spectra obtained for the products mentioned in this work, in the 4000-300 cm^{-1} range, were recorded as solids with a Perkin Elmer FT-IR Paragon 1000 spectrophotometer with a single-reflection diamond ATR P/N 10500. X-band powder EPR spectra were obtained on a Bruker-EMXplus electron spin resonance spectrometer (Field calibrated with DPPH ($g = 2.0036$))

F. Cytotoxicity and IC_{50} determination. The *in vitro* cytotoxicity test of compounds L1, and RuL1 were performed using the SRB test [63] for estimation of cell viability. The human cell lines MCF-7 (breast cancer), EVSA (breast cancer), WIDR (colon cancer), IGROV (ovarian cancer), M19-MEL (melanoma cancer), A498 (renal cancer) and H226 (non-small cell lung cancer) were used. Cell lines WIDR, M19 MEL, A498, IGROV and H226 belong to the currently used anticancer screening panel of the National Cancer Institute, USA [64]. The MCF-7 cell line is an oestrogen receptor (ER)⁺/ progesterone receptor (PgR)⁺ and the cell line EVSA-T is (ER)⁻/ PgR)⁻. Prior to the experiments a mycoplasma test was carried out on all cell lines and found to be negative. All the cell lines were maintained in a continuous logarithmic culture in RPMI 1640 (Invitrogen, Paisley Scotland) medium with Hepes and phenol red. The medium was supplemented with 10% foetal calf serum (Invitrogen, Paisley Scotland), penicillin 100 IU/mL (Sigma, USA) and streptomycin 100 $\mu\text{g}/\text{mL}$ (Sigma, USA). The cells were mildly trypsinized for passage and for use in the experiments. For the cell growth assay, cells (1500-2000 cells/150 μl of complete medium/well) were pre-cultured in 96 multi-well plates (falcon 3072, BD) for 48 h at 37 $^{\circ}\text{C}$ in a 5% CO_2 containing incubator and subsequently treated with the tested compounds for 5 days. The stock solutions of the compounds were prepared in the corresponding medium. A three-fold dilution sequence of ten steps was made in full medium, starting with the 250000 ng/mL stock solution. Every dilution was used in quadruplicate by adding 50 μL to a column of wells. The result in the highest concentration of 62500 ng/mL is present in column 12. Column 2 was used for the blank and column 1 was completed with medium to diminish interfering evaporation. After a 120 h incubation time, the surviving cells in cultures, treated with the compounds were detected, using the sulforhodamine B (SRB, sigma, USA) test [63]. After the incubation time cells were fixed with 10% of trichloroacetic acid (sigma, USA) in PBS (Emmer-Compascuum, NL). After three washing cycles with tap water, the cells were stained for at least 15 minutes with 0.4% SRB dissolved in 1% of acetic acid (Baker BV, NL). After staining, the cells were washed with 1% acetic acid to remove the unbound stain. The plates were air-dried and the bound stain was dissolved in 150 μL of 10mM Tris-base (tris(hydroxymethyl)aminomethane). The absorbance was read at 540 nm using an automated microplate reader (Labsystems Multiskan MS). Data were used for construction of concentration-response curves and determination of the ID_{50} values was graphically done by use of Deltasoft 3 software. The variability of the *in vitro* cytotoxicity test depends on the cell line used and the serum applied. With the same batch of cell lines and the same batch of serum the inter-experimental CV (coefficient of variation) is 1-11% depending on the cell line and the intra-experimental CV is 2-4%. These values may be higher when using other batches of cell lines and/or serum.

4.2.2 Synthetic procedures

All the chemicals and analytical grade solvents were purchased from various commercial sources and were used without further purification treatments unless otherwise stated. Ruthenium trichloride hydrate was a generous gift from Johnson Matthey, UK. All synthesized compounds are reasonably thermally stable and air-stable, both in the solid state and in solution. For caution's sake, however, their preparation and manipulation in solution were carried out under an inert atmosphere (Ar).

A. Synthesis of 2,6-pyridinedicarboxaldehyde. The synthetic procedure has been reported previously by Papadopolous [65] and was later modified by Vance [66]. Activated manganese(IV) dioxide (Across) was prepared by heating overnight at 110 °C. An excess of MnO₂ (100 g) and 10.0 g (71.9 mmol) of 2,6-bis(hydroxymethyl)pyridine (Aldrich) were refluxed with stirring for 5 h in 500 mL of chloroform (Biosolve, spectrophotometric grade). The oxide residue was separated from the solution by vacuum filtration and the black residue was rinsed four times with 100 mL of chloroform. Solvent was removed from the solution by rotary evaporation, and then the crude product was dissolved in the minimal amount of chloroform and passed through a silica gel column (ca. 15 cm long, ca. 4 cm diameter). The pure dialdehyde elutes easily and can be seen as an opaque white band in the clear silica gel, while impurities remain at the top of the column. Removal of the solvent by rotary evaporation gives the product in 59% yield; mp = 114-118 °C. ¹H NMR spectrum (400 MHz, chloroform, 294 K, s=singlet, d=doublet, t=triplet and m=multiplet): 10.1782 (s, CH, 2H), 8.1975 (d, pyH, 2H), 8.0912 (t, pyH, 1H) ppm.

B. Synthesis of 2,6-bis(2,4,6-trimethylphenyliminomethyl)pyridine, L1. The procedure followed was previously reported by Balamurugan [40]. To a solution of 2,6-pyridinedicarboxaldehyde (0.68 g, 5.0 mmol) in absolute methanol (25 mL) (Biosolve), were successively added 2,4,6-trimethylaniline (Aldrich) (1.35 g, 10.0 mmol) and the resulting mixture was refluxed for 2 h over molecular sieves (4 Å). The reaction mixture was filtered while hot. Upon cooling, a yellow crystalline solid (L1), was obtained in high yield (1.7736 g, 96%). Diffraction-quality crystals were grown from dmf. Elemental analysis for C₂₅H₂₇N₃: Calculated (%): C, 81.26; N, 11.37; H, 7.36. Found (%): C, 81.20; N, 11.47; H, 7.64. ESI-MS: m/z=465.23, [(C₂₅H₂₈N₃)(CH₃CN)(H₂O)₃]¹⁺, where calculated m/z=465.61. IR: 3100-2800, 1640-1565, 1481, 1451-1430, 1205, 1139, 852, 815, 733, 642, 588-573 and 384 cm⁻¹. UV-Vis in dmf (λ_{max}(logε_M)): 300.1(3.67) and 356(3.69). ¹H NMR (300 MHz, dmf, 294 K, s=singlet, d=doublet, t=triplet and m=multiplet): δ=8.43(d, 2H, H₂ and H_{2a}), 8.41(s, 2H, H₄ and H_{4a}), 8.23(t, 1H, H₃), 6.93(s, 4H, H₇, H_{7a}, H₉ and H_{9a}), 2.26(s, 6H, 3H₁₂ and 3H_{12a}) and 2.12 ppm (s, 12H, 3H₁₁, 3H_{11a}, 3H₁₃ and 3H_{13a}).

C. Synthesis of 2,6-bis(2,6-diisopropylphenyliminomethyl)pyridine, L2. The procedure followed was previously reported by Britovsek *et al.*, [67] and modified by Balamurugan *et al.*, [40]. To a solution of 2,6-pyridinedicarboxaldehyde (0.68 g, 5.0 mmol) in absolute ethanol (25 mL) (Biosolve), were successively added 2,6-diisopropylaniline (Aldrich) (1.77 g, 10.0 mmol) and one drop of glacial acetic acid and then the resulting mixture was refluxed over molecular sieves(4Å). After 24h under reflux, the solution was filtered while hot and the ligand (L2) (1.907 g, 84.1%) was obtained after cooling down the filtrate. Diffraction-quality crystals were grown from dmf. Elemental analysis for C₃₁H₃₉N₃: Calculated (%): C, 82.07; N, 9.26; H, 8.66. Found (%): C, 82.02; N, 9.36; H, 8.90. ESI-MS: m/z=454.33, [C₃₁H₄₀N₃]¹⁺, where calculated m/z=454.68; m/z=549.38, [(C₃₁H₄₀N₃)(CH₃CN)(H₂O)₃]¹⁺, 100%, where calculated m/z=549.78. IR: 3000-2850, 1636-1560, 1456, 1451-1448, 1184, 992, 931, 870-850, 824-714, 526 and 453 cm⁻¹. UV-Vis in dmf (λ_{max}(logε_M)): 285 (4.02) and 352(3.42). ¹H NMR (300 MHz, dmf, 294 K, s=singlet, d=doublet, t=triplet and m=multiplet): δ=8.47(d, 2H, H₂ and H₄), 8.42(s, 2H, H₆ and H₁₉), 8.29(t, 1H, H₃), 7.17(m, 6H, H₉, H₁₀, H₁₁, H₂₂, H₂₃, and H₂₄), 2.97(m, 4H, H₁₃, H₁₆, H₂₆ and H₂₉) and 1.15 ppm (d, 24H, 3H₁₄, 3H₁₅, 3H₁₇, 3H₁₈, 3H₂₇, 3H₂₈, 3H₃₀ and 3H₃₁).

D. Synthesis of 2,6-bis(4-methylphenyliminomethyl)pyridine, L3. The procedure followed for the synthesis of this compound resembles the previous synthetic procedures. 2,6-pyridinedicarboxaldehyde (0.68 g, 5.0 mmol) and 4-methylaniline (Aldrich) (1.0717g, 10.0 mmol) were refluxed in absolute methanol (25 mL) (Biosolve) for 6 h over molecular sieves(4Å). The

reaction mixture was filtered while hot. Upon cooling, a yellow crystalline solid (L3), was obtained, filtered, washed and dried (1.1654 g, 74.38%). Diffraction-quality crystals were grown from dmf. Elemental analysis for $C_{21}H_{19}N_3$: Calculated (%): C, 80.48; N, 13.41; H, 6.11. Found (%): C, 79.60; N, 13.49; H, 5.89. ESI-MS: $m/z=313.94$, $[C_{21}H_{20}N_3]^{1+}$, where calculated $m/z=314.41$; $m/z=335.95$, $[(C_{21}H_{20}N_3)_2(CH_3CN)]^{2+}$, where calculated $m/z=334.94$; $m/z=376.92$, $[(C_{21}H_{20}N_3)_2(CH_3CN)_3]^{2+}$, 100%, where calculated $m/z=375.98$. IR: 3100-2800, 1624-1565, 1505, 1464, 1339, 1201, 1139, 958-949, 817, 738, 632, 544-490 and 440 cm^{-1} . UV-Vis in dmf ($\lambda_{max}(\log\epsilon_M)$): 327(4.34). 1H NMR (300 MHz, dmf, 294 K, s=singlet, d=doublet, t=triplet and m=multiplet): $\delta=8.74$ (s, 2H, H_5 and H_{5a}), 8.32(d, 2H, H_3 and H_{3a}), 8.19(t, 1H, H_4), 7.34(m, 8H, H_8 , H_{8a} , H_9 , H_{9a} , H_{11} , H_{11a} , H_{12} and H_{12a}) and 2.37 ppm (s, 6H, $3H_{13}$ and $3H_{13a}$).

E. Synthesis of 2,6-bis(phenyliminomethyl)pyridine, L4. The procedure followed was previously reported by Lions [49]. A mixture of 2,6-pyridinedicarboxaldehyde (0.20 g, 1.5 mmol), aniline (Aldrich) (0.28 g, 3.0 mmol), one drop of concentrated sulphuric acid (Riedel-deHaen) and 150 mL of absolute methanol (Biosolve), was stirred under argon atmosphere at room temperature for 16 h over molecular sieves(4Å). The solvent was removed by rotary evaporation and the residue was recrystallized from acetonitrile (0.16 g, 38%). Elemental analysis for $C_{19}H_{15}N_3$: Calculated (%): C, 79.98; N, 14.73; H, 5.30. Found (%): C, 79.13; N, 14.66; H, 5.61. ESI-MS: $m/z=285.96$ $[C_{19}H_{16}N_3]^{1+}$, where calculated $m/z=286.36$; $m/z=307.98$, $[(C_{19}H_{16}N_3)_2(CH_3CN)]^{2+}$, where calculated $m/z=306.88$; $m/z=348.98$, $[(C_{19}H_{16}N_3)_2(CH_3CN)_3]^{2+}$, 100%, where calculated $m/z=347.94$. IR: 3100-2800, 1628, 1592-1560, 1484, 1336, 1202, 1074, 994-855, 816, 758-736, 692, 644, 518 and 315 cm^{-1} . UV-Vis in dmf ($\lambda_{max}(\log\epsilon_M)$): 313(4.33). 1H NMR (300 MHz, $CDCl_3$, 294 K, s=singlet, d=doublet, t=triplet and m=multiplet): $\delta=8.69$ (s, 2H, H_5 and H_{5a}), 8.30(s, 2H, H_3 and H_{3a}), 7.95(t, 1H, H_4) and 7.34ppm(s, 10H, H_{8-12} , H_{8a-12a}).

F. Synthesis of trichlorido(2,6-bis(2,4,6-trimethylphenyliminomethyl)pyridine)ruthenium(III) hydrate, RuL1. 0.1g (0.382 mmol) of $RuCl_3 \cdot 3H_2O$ (Johnson Matthey Chemicals) was dissolved in an ethanolic solution (ethanol/water, 3:2) (Riedel-deHaen) and was gently refluxed at 109 °C with continuous purging of argon for 4.5 h. After that, the hot reaction mixture was cooled to RT. The resulting solution was filtered through a glass filter and placed in a new round-bottom flask. Then 0.6 mL of concentrated HCl (Riedel-deHaen) and 0.1483 g (1.05 eq, 0.4014 mmol) of L1 was added. The reaction mixture was further refluxed for 2 h and cooled down and again stirred for further 12 h at RT. The dark-brown solid formed after this time was collected by filtration, washed with plenty of cold dichloromethane, cold ethanol, and cold water and finally dried with dry diethyl ether. Yield: 92 % (0.3514 mmol, 0.2090 g). Elemental analysis for $RuC_{25}H_{27}N_3Cl_3 \cdot (H_2O)$: Calculated (%): C, 50.47; N, 7.06; H, 4.91. Found (%): C, 50.37; N, 7.05; H, 5.03. ESI-MS: $m/z=582.07$, $[Ru(C_{25}H_{27}N_3)Cl_2CH_3CN]^{1+}$, where calculated $m/z=582.44$. IR: 3050-2860, 1595.5, 1476-1440, 1377, 1334, 858.6, 606.8, 452.1 374.3 and 326 cm^{-1} . UV-Vis in dmf ($\lambda_{max}(\log\epsilon_M)$): 317(3.74), 390(3.80), 482(3.40) and 594(3.1). 1H NMR (300 MHz, dmf, 294 K, s=singlet, d=doublet, t=triplet and m=multiplet): $\delta=4.636$ (s, 4H, H_7 , H_{7a} , H_9 and H_{9a}), 1.5983(s, 6H, $3H_{12}$ and $3H_{12a}$), -1.850 (broad s, 2H, H_2 and H_{2a}), -2.417 (broad s, 12H, $3H_{11}$, $3H_{11a}$, $3H_{13}$ and $3H_{13a}$), -4.291(broad s, 1H, H_3) and -27.850 ppm (broad, 2H, H_4 and H_{4a}).

G. Synthesis of trichlorido(2,6-bis(2,6-diisopropylphenyliminomethyl)pyridine)ruthenium(III), RuL2. 0.05g (0.191 mmol) of $RuCl_3 \cdot 3H_2O$ (Johnson Matthey Chemicals) was dissolved in an ethanolic solution (ethanol/water, 3:2) (Riedel-deHaen) and was gently refluxed at 109 °C with continuous purging of argon for 4 h. After that, the hot reaction mixture was cooled to RT. The resulting solution was filtered through a glass filter and placed in a new round-bottom flask. Then 0.3 mL of concentrated HCl (Riedel-deHaen) and 0.091 g (1.05 eq, 0.4014 mmol) of L2 was added. The reaction mixture was further refluxed for 2h and cooled down and again stirred for further 24 h at RT. The dark-brown solid formed after this time was collected by filtration, washed with plenty of cold dichloromethane, cold ethanol, and cold water and finally dried with dry diethyl ether. Yield: 81 % (0.1543 mmol, 0.102 g). Elemental analysis for $RuC_{31}H_{39}N_3Cl_3$: Calculated (%): C, 56.32; N, 6.36; H, 5.95. Found (%): C, 56.19; N, 6.40; H, 6.26. ESI-MS: $m/z=666.18$, $[Ru(C_{31}H_{39}N_3)Cl_2(CH_3CN)]^{1+}$, where calculated $m/z=666.70$. IR: 3050-2800, 1456,

1362-1331, 1162, 1059, 958-898, 803-746, 593, 390 and 326 cm^{-1} . UV-Vis in dmf ($\lambda_{\text{max}}(\log \epsilon_{\text{M}})$): 293(3.78), 387(3.72), 509(3.47) and 613(3.01). ^1H NMR (300 MHz, dmf, 294 K, s=singlet, d=doublet, t=triplet and m=multiplet): δ =4.93(s, 4H, H₉, H₁₁, H₂₂ and H₂₄), 0.57(s, 2H, H₁₀ and H₂₃), -1.24 (broad s, 24H, 3H₁₄, 3H₁₅, 3H₁₇, 3H₁₈, 3H₂₇, 3H₂₈, 3H₃₀ and 3H₃₁), -1.90(broad s, 2H, H₂, and H₄), -4.25(broad s, 1H, H₃), -6.40(broad s, 4H, H₁₃, H₁₆, H₂₆ and H₂₉), and -28.53 ppm (broad, 2H, H₆ and H₁₉).

H. Synthesis of aquobis(9-ethylguanine)(2,6-bis(2,4,6-trimethylphenyliminomethyl)pyridine)ruthenium(II) perchlorate, RuL1-2(9EtGua). This compound was synthesized by the procedure described by van Vliet [39] for Ru(tpy)(9EtGua)₂(PF₆)₂ synthesis, with minor modifications: 30 mg (0.0504 mmol) of RuL1 and 27.11 mg (3 Eq, 0.1513 mmol) of 9-ethylguanine were dissolved in 6 mL ethanol/water (70:30). The reaction mixture was kept under reflux for 24 h. After reflux, the volume of the solution was reduced by a half by rotary evaporation and 1.5 mL of aqueous saturated NaClO₄ solution was added. After two days the formed solid was collected by filtration, washed with plenty of cold water, cold chloroform and dried with dry diethyl ether. Yield: 70.85 % (0.03571 mmol, 37.36 mg). X-ray quality crystals were obtained by slow evaporation of a concentrated solution of RuL1-2(9EtGua) in methanol. Elemental analysis for RuC₃₉H₄₇N₁₃Cl₂O₁₁: Calculated (%): C, 44.79; N, 17.41 and H, 4.53. Found (%): C, 44.82; N, 17.28 and H, 4.78. ESI-MS: m/z =946.75, [RuL1-2(9EtGua) - 1ClO₄]⁺, where calculated m/z =946.41; m/z =927.74, [RuL1-2(9EtGua) - 1H₂O - 1ClO₄]⁺, where calculated m/z =928.39; m/z =434.73, [RuL1-2(9EtGua) + 1H₂O - 2ClO₄]²⁺, where calculated m/z =432.47 and m/z =413.80, [RuL1-2(9EtGua) - 1H₂O - 2ClO₄]²⁺, 100%, where calculated m/z =414.47. IR: 3340, 3200-2900, 1661, 1634.4, 1603.5, 1568-1423, 1081.5, 622 and 374 cm^{-1} . UV-Vis in methanol ($\lambda_{\text{max}}(\log \epsilon_{\text{M}})$): 317(4.01), 363(3.93), 477(3.76) and 552(3.2). ^1H NMR (300 MHz, methanol, 294 K, s=singlet, d=doublet, t=triplet and m=multiplet): δ =8.44(s, 2H, H₄ and H_{4a}), 8.40(d, 2H, H₂ and H_{2a}), 8.06(t, 1H, H₃), 6.77(s, 4H, H₇, H_{7a}, H₉ and H_{9a}), 6.68(s, 2H, H₁₈ and H_{18a}), 4.61(broad s, 4H, N₅-H), 3.94(m, 4H, 2H₁₉ and 2H_{19a}) 2.22(s, 6H, 3H₁₂ and 3H_{12a}), 1.32(s, 12H, 3H₁₁, 3H_{11a}, 3H₁₃ and 3H_{13a}) and 1.17 ppm (t, 6H, H₂₀ and H_{20a}).

Caution: perchlorate salts of metal complexes with organic ligands are potentially explosive. Only small amounts of the compound should be prepared and handled with great care.

4.3 Results and discussion

4.3.1 Synthesis and characterization of the bis(arylimino)pyridine ligands

The series of ligands was selected with the aim to obtain information in regard to the influence of the ligand electronic and steric factors in the Ru(III) compounds anticancer activity. The preparation of the bis(arylimino)pyridine ligands, L1, L2, L3 and L4 was achieved applying reported procedures or procedures with small modifications and all of them are described in the experimental section. Condensation of 1 equiv. of 2,6-bis(aldehyde)pyridine with 2 equiv. of the required aniline [42] to produce 2,6-bis(arylimino)pyridine ligands is the most commonly used synthetic procedure. A few earlier results have been reported [47, 67, 68] related to the rich chemistry developed by these bis(imino)pyridine ligands, which is result of the many favourable reactive sites (figure 4.1), including the nitrogen and carbon centres of the imine moiety as well as the pyridine ring. Little attention has been given to changes of the substituents at the imine carbon, although most of the earlier research has been directed to bis(imino)pyridine frame modifications in the groups attached to the imino nitrogen [47]. Some synthetic strategies for the preparation of bis(imino)pyridine derivatives with different symmetry are known; for instance, the method of reacting 2,6-bis(acetyl)pyridine, first, with 1 equiv. of a substituted aniline and subsequently with 1 equiv. of either a primary amine or a different aniline has been successfully applied in the synthesis of (2-arylimino-6-alkylimino)pyridines or 2,6-bis(arylimino)pyridines [42, 69-71]. Variable substitution patterns on the aryl rings bound to the imine nitrogen atoms can easily be obtained, as well as different substituents located in the pyridine moiety. For instance, the introduction of a bulky alkyl group at the 4 position in the pyridine ring (*para* with respect to the nitrogen atom) that can impair a better hydrophobic nature could be easily obtained through a radical attack [72], or to double the 2,6-bis(imino)pyridyl moiety to give polydentate ligands (6N) capable of coordinating two metal centres [73]. All these possibilities clearly underline the facile

tunability of the chemical and physical properties of the ligands by themselves, but also of the coordination compounds formed with them, which finally will be reflected in the cytotoxicity. The 2,6-bis(aryliminomethyl)pyridine ligands (figure 4.2), used in the synthesis of the Ru(III) compounds discussed here, were prepared in one single step with high yields from the condensation of two equivalents of the proper aniline with one equivalent of 2,6-pyridinedicarboxaldehyde (Figure 4.4).

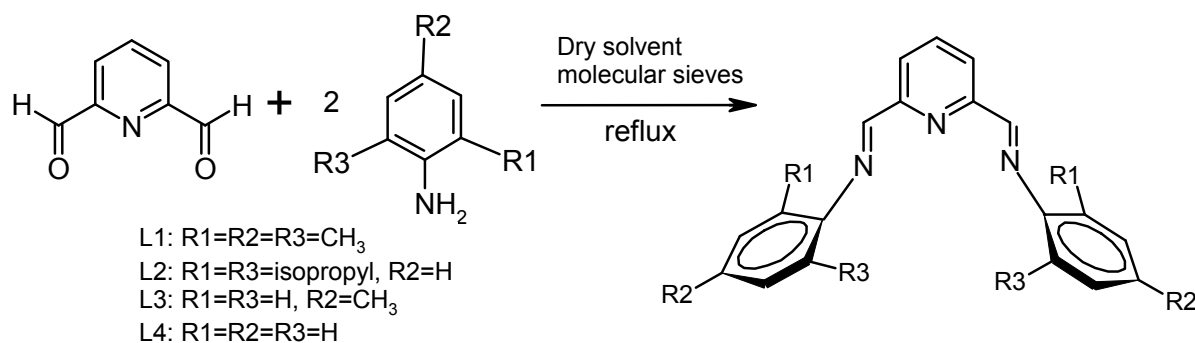


Figure 4.4 Schematic representation of the synthesis of L1-L4.

All four 2,6-bis(arylimino)pyridine derivatives synthesised were found to be air-stable and soluble in common organic solvents. L1-L4 were fully characterized by elemental analysis, ¹H NMR, mass spectroscopy, and IR and UV-Vis studies as well, and the results agree with data previously reported. In addition, L1, L2 and L3 were studied by X-ray diffraction studies (selected data are included in Appendix A). For all cases, the spectroscopic properties are in accordance with their formulation and the relevant data are summarize in table 4.1 and the numbering corresponding to the ¹H NMR assignment is presented in figure 4.5.

All the ligands display molecular ion envelopes of high to medium intensity in their positive ESI mass spectra, confirming the nature of all compounds. Characteristic trends in the fragmentation patterns of the ligands can be observed (table 4.1). Fragmentation ions interacting with solvent molecules could be proposed, as well as the presence of starting materials ions. All the peaks exhibited the correct isotopomer distribution.

IR spectra of L1-L4 displayed characteristic frequencies in the range 4000-400 cm⁻¹ (table 4.1). The functional groups, C=N(imino), C=C and C=N(pyridine) stretching modes were observed in this range. From IR data, a shift to lower frequencies for the C=N(imino) bond stretching vibration is observed when comparing the gradual reduction in the number of methyl groups in the aryl moieties. Then the C=N(imino) stretching band has a high frequency value when electron-donating groups are in conjugation. A typical conjugated C=N stretching band appears as a sharp peak around 1640 cm⁻¹ [74-77]. The intensity of this stretching vibration is larger when comparing with the C=C stretching vibration because of the C-N polarity.

Table 4.1 Spectroscopic data for the ligands.

Ligand	IR (ν C=N, cm ⁻¹) ^a	¹ H NMR ^b	ESI-MS (m/z) ^c
L1	1640	8.43(d, 2H, H ₂ , H _{2a}), 8.41(s, 2H, H ₄ , H _{4a}), 8.23(t, 1H, H ₃), 6.93(s, 4H, H ₇ , H _{7a} , H ₉ , H _{9a}), 2.26(s, 6H, 3H ₁₂ , 3H _{12a}) and 2.12 ppm (s, 12H, 3H ₁₁ , 3H _{11a} , 3H ₁₃ , 3H _{13a})	465.23(465.61)
L2	1636	8.47(d, 2H, H ₂ , H ₄), 8.42(s, 2H, H ₆ , H ₁₉), 8.29(t, 1H, H ₃), 7.17(m, 6H, H ₉ , H ₁₀ , H ₁₁ , H ₂₂ , H ₂₃ , H ₂₄), 2.97(m, 4H, H ₁₃ , H ₁₆ , H ₂₆ , H ₂₉) and 1.15 ppm (d, 24H, 3H ₁₄ , 3H ₁₅ , 3H ₁₇ , 3H ₁₈ , 3H ₂₇ , 3H ₂₈ , 3H ₃₀ , 3H ₃₁)	454.33(454.68) 549.38(549.78)
L3	1624	8.74(s, 2H, H ₅ , H _{5a}), 8.32(d, 2H, H ₃ , H _{3a}), 8.19(t, 1H, H ₄), 7.34(m, 8H, H ₈ , H _{8a} , H ₉ , H _{9a} , H ₁₁ , H _{11a} , H ₁₂ , H _{12a}) and 2.37 ppm (s, 6H, 3H ₁₃ , 3H _{13a})	313.94(314.41) 335.95(334.94) 376.92(375.98)
L4	1628	8.69(s, 2H, H ₅ , H _{5a}), 8.30(s, 2H, H ₃ , H _{3a}), 7.95(t, 1H, H ₄) and 7.34ppm(s, 10H, H ₈₋₁₂ , H _{8a-12a})	285.96(286.36) 307.98(306.88) 348.98(347.94)

^a Solid, imino group ^b In DMF deuterated, 294 K, s=singlet, d=doublet, t=triplet and m=multiplet, ^c Simulated masses are presented in parenthesis

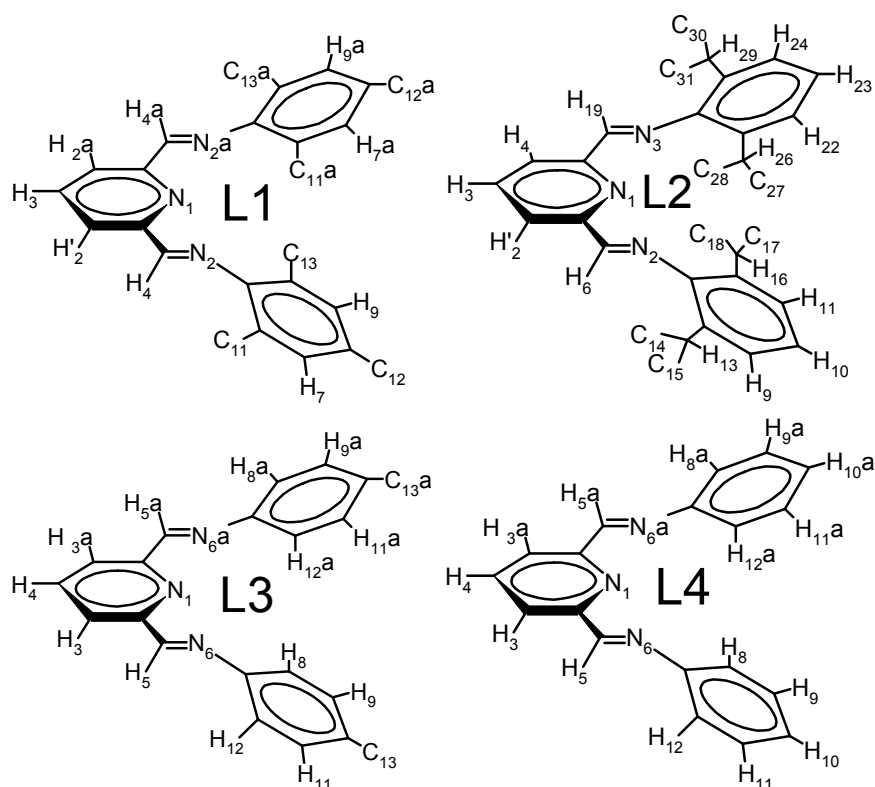


Figure 4.5 Schematic representation of 2, 6-bis(arylimino)pyridine ligands synthesized with the numbering used in the assignment of the resonance peaks. Hydrogen atoms in the methyl moieties have been omitted for clarity.

The strong C=N(pyridine) bond stretching vibrations are detected around 1580 cm^{-1} , although no relevant shifts in these stretching vibrations frequencies are observed among the ligands. Upon coordination important shifts are expected to be observed due to the participation of the pyridine ring in coordination with the metal. In fact, it has been reported that upon complex formation, the pyridine vibrations in the high frequency region are not appreciably shifted, whereas those at 600 cm^{-1} (in-plane ring deformation) (ρ_{pyridine}) and 500 cm^{-1} (out-of-plane ring deformation) ($\rho_{\text{out pyridine}}$) are shift to higher frequency [78]. Other important peaks related to the aromatic nature of these ligands are located in the frequency range of $790\text{--}650\text{ cm}^{-1}$. The pattern of substitution in the aromatic rings could be described by the peaks located in this range. The assignment of selected bands and frequencies are summarized in table 4.2.

Table 4.2 IR assignment of selected peaks in 2,6-bis(arylimino)pyridine ligands.

Peaks	Frequencies (cm^{-1})			
	L1	L2	L3	L4
ν (C=N)imino	1640	1636	1624	1628
ν (C=N)pyridine	1565	1587-1560	1575	1591
ν (C=C)	1481-1451	1456-1445	1501-1464	1484-1460
ρ_{pyridine}	643	668	632	644
$\rho_{\text{out pyridine}}$	506	526	517	518
aryl substitution	852-815	866-714	873-708	816-692

One of the most powerful spectroscopic methods for the structural determination of these organic molecules is the NMR. The ^1H NMR spectra from the ligands discussed here, the corresponding assignment of peaks and general data are condensed in figure 4.6 and table 4.1. From the ^1H NMR spectra, several patterns are observed. In all cases, the clean spectra indicate a high purity of the samples. The assignment of each peak was obtained through the integration values, multiplicity of signals, deshielding effect in the hydrogen atoms close to the nitrogen atom in the pyridine ring and 2D ^1H COSY experiments. Due to the symmetry in these molecules, the spectra are relatively simple (figure 4.6).

The relevant feature of these ^1H NMR spectra, is the appearance of four sets of hydrogen atom resonances corresponding to the protons in the pyridine ring, the aryl ring, the imino- and the methyl-aryl moieties. For each of the four ligands, the set of protons corresponding to the pyridine

ring appear in the range of 7.9-8.5 ppm, showing the expected multiplicity and integration values (table 4.1 and figure 4.6). The resonance peaks are located in the downfield region of the spectra due to the electronegativity of the nitrogen in the heterocyclic structure. The resonance peaks, in the spectral region from 6.8-7.4 ppm, corresponding to the aryl protons, present the expected multiplicity and integration values as well [40, 49, 67, 79].

The signals for the imino protons (H-C=N) appear as singlets. They are observed in the region 8.7-8.3 ppm which is typical for this group [79-82]. There is an upfield shift for this signal with the increasing electron releasing nature of the aryl rings, directly connected through the imino nitrogen. The more methyl substitution is present in the aryl ring, the more upfield shift effect.

The methyl moieties in the aryl ring, at the *para* position, show a resonance peak in the range 2.2-2.4 ppm, as seen in the ^1H NMR spectra of L1 and L3. The methyl and isopropyl moieties localized in the *ortho* position are magnetically equivalent and show a resonance peak in the higher field region of the spectra. The multiplicity observed for the isopropyl-resonance peak, could be explained due to the coupling with the hydrogen atom bound to the carbon atom directly connected to the aryl ring.

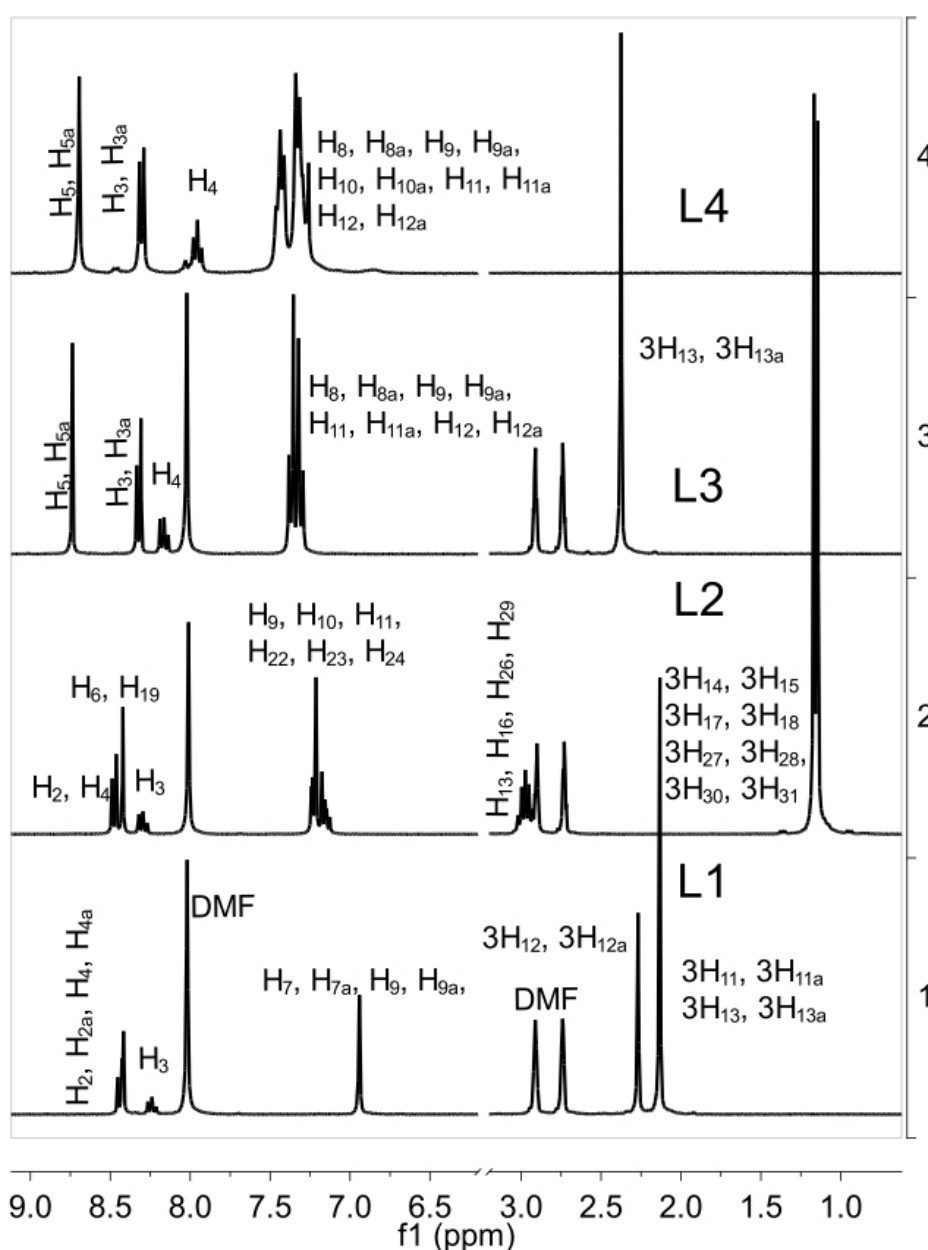


Figure 4.6 ^1H NMR spectra of all the 2,6-bis(arylimino)pyridine ligands synthesised and characterized. L1, L2 and L3 spectra are measured in deuterated dmf, while L4 is measured in deuterated chloroform. Numbering describing the assignments could be consulted in figure 4.5.

The absorption spectra of all the 2,6-bis(arylimino)pyridine ligands in the UV-Vis region were recorded using a Varian CARY 50 UV/VIS spectrophotometer operating at room temperature. The electronic spectra had to be recorded in freshly prepared dmf solutions, due to the poor solubility in water. The UV and Visible absorption spectra of the compounds under investigation display one or two bands in dmf within the range 270-400 nm. The UV-Vis spectra of all compounds are essentially consisting of $\pi \rightarrow \pi^*$ -transitions in the range 270-400 nm with high molar absorption coefficients. The detailed information is fully described in the experimental section and the UV-Vis spectra of the ligands are depicted in figure 4.7 and condensed data in table 4.3. The first band, at 250-300 nm could be assigned to the moderate energy $\pi \rightarrow \pi^*$ -transition of the aromatic rings, while the second band 310-360 nm is due to the low $\pi \rightarrow \pi^*$ -transition of the azomethine group [82].

Important to notice again is the influence of the methyl moieties attached to the aryl rings in the electronic spectra. When the methyl group is attached to the aryl moiety, at *ortho* and/or *para* position, a significant bathochromic shift is observed in the intraligand charge-transfer transitions, as clearly visible in the case of L1 and L2 when comparing with unsubstituted L4 or partially substituted L3 (*para* substitution). This effect may be explained as a result of the increased π -electron density, although interactions with the solvent could not be discharged. The increase in electron density in the ligands generates a moderate decrease in the molar absorption coefficient, particularly higher in the transitions of the imine group (table 4.3).

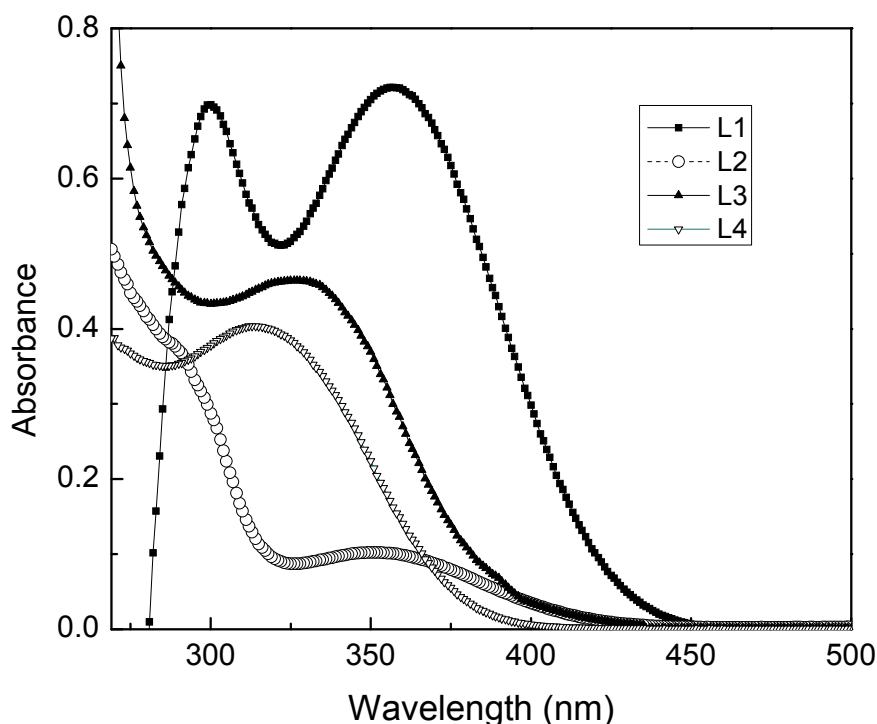


Figure 4.7 UV-Vis spectra of L1, L2, L3 and L4 in dmf at 294 K; [L1]=0.148mM, [L2]=0.037mM, [L3]=0.0213mM and [L4]=0.0187mM.

Table 4.3 Electronic spectral data for the 2,6-bis(arylimino)pyridine ligands.

Transitions nature	Wavelength [$\log \epsilon_m$] (nm)			
	L1	L2	L3	L4
$\pi \rightarrow \pi^*$	300.1[3.67]	285[4.02]	-	-
$\pi \rightarrow \pi^*$	356[3.69]	352[3.42]	327[4.34]	313[4.33]

Slow diffusion of water in concentrated dmf solutions of the ligands produced crystals that were suitable for diffraction studies and confirmed the structures depicted with data obtained from the other characterization techniques. Figures 4.8-4.10 present the molecular structure of ligands L1, L2 and L3. The crystallographic data, selected bond distances and angles are given in Appendix A. All bond length and angles have comparable numbers is related organic structures.

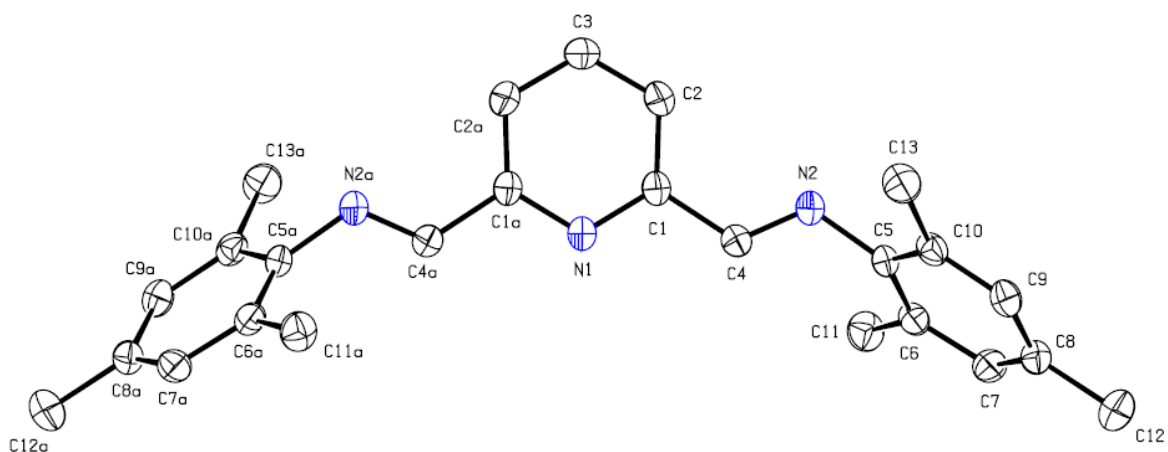


Figure 4.8 Molecular structure of the asymmetric unit of L1 and atom numbering.

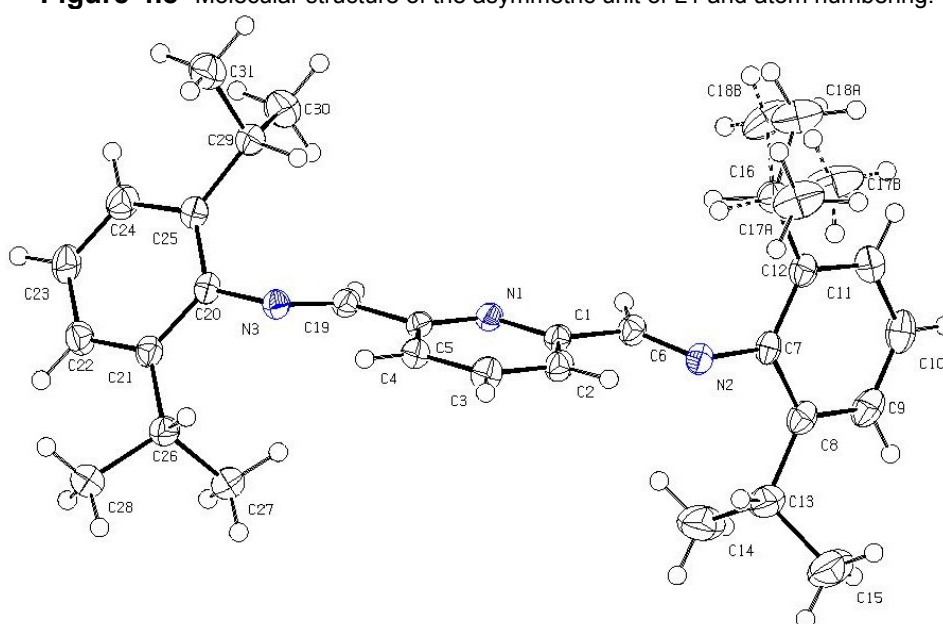


Figure 4.9 Molecular structure of the asymmetric unit of L2 and atom numbering.

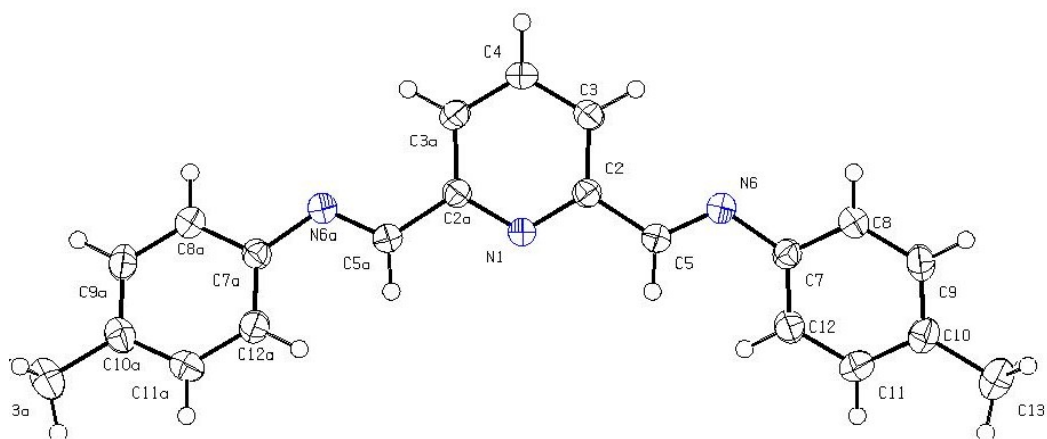


Figure 4.10 Molecular structure of the asymmetric unit of L3 and atom numbering.

4.3.2 Synthesis and characterization of bis(arylimino)pyridine-Ru(III) compounds

The compounds of formula $[\text{RuCl}_3(\text{L})] \cdot x(\text{H}_2\text{O})$, where $\text{L}=\text{L}1=2,6\text{-bis}(2,4,6\text{-trimethylphenyl-iminomethyl})\text{pyridine}$, $\text{L}2=2,6\text{-bis}(2,6\text{-isopropylphenylimino methyl})\text{pyridine}$ and $x=0$ or 1 (abbreviated as $\text{RuL}1$ and $\text{RuL}2$ respectively) were synthesized in good yields by treating

RuCl₃·3H₂O with the corresponding ligand in a refluxing ethanol:water mixture. Despite promising catalytic properties and increased attention to the study of such metal-ligand systems [45], attempts to synthesize Ru compounds with 2,6-bis(imino)pyridine ligands and different starting Ru compounds have remained largely unsuccessful [83]; in fact only one related Ru compound has so far been described in the literature [83, 84]. The establishment of the best experimental conditions described in this thesis was achieved through several experiments and analysis of the products. The reactions described here, present remarkable high yields (80-90%), contrary to procedures previously reported in the literature [83, 84]. The isolation of solids (neutral compounds), due to the presence of an excess of chloride ions (HCl), must be the key factor for these high yield results.

Applying the same experimental conditions for the isolation of Ru(III) derivatives of L3 and L4 (the less bulky ligands), has remained unsuccessful, probably due to redox processes and formation of several by-products like the bis-chelate derivatives of Ru(II). Such a behaviour has been observed for the related 2,6-bis(arylimino)pyridine-Fe(III) system [85]. In this iron system, it appears that the formation of mono- *versus* bis-chelate complexes is anion dependent, as was noted previously for the FeCl₂ vs. FeBr₂ compounds of bis(imino)pyridine ligands containing small substituents in the imino moiety, such as phenyl and also for terpyridine iron(II) compounds [44, 49, 85, 86]. Only in the case of sufficiently bulky 2,6-disubstituted phenyl groups, bis-chelate formation could be prevented completely. Further attempts in the synthesis of Ru(III)L3 and Ru(III)L4 compounds were then postponed as a wide range of possibilities were immediately suggested just for RuL1 and RuL2; therefore the following discussion comprises these last 2 Ru(III) derivatives.

Ruthenium monoterpyridine complexes have received considerable research attention primarily due to their strong metal to ligand charge transfer transitions, facile electron-transfer properties and long-lived ³MLCT excited states and these in combination make them attractive for designing photo- and electrochemical devices [87-92]. It is of particular interest that the electronic nature of the ancillary functions in the ruthenium monoterpyridine core plays an important role in directing their chemical and electrochemical properties

The 2,6-bis(arylimino)pyridine ligands, described in this project, are symmetric heteroaromatic tridentate ligands, which coordinate through the pyridine and imino nitrogen atoms, forming stable five-membered chelating rings (see Figure 4.3). 2,6-bis(arylimino)pyridine ligands are considered capable of acting both as σ -donor and as π -acceptor. The pyridine ring contributes with its intermediate π -acceptor properties, while its nitrogen is a relatively weak σ -donor. The imino group has a reduced σ -donor ability, but possesses enhanced π -accepting properties through the imino π^* -orbital. The nitrogen of the pyridine ring in these 2,6-bis(arylimino)pyridine ligands resembles the coordinating properties of the pyridine group in the closely related ligand terpyridine, which means that the nitrogen is a weak σ -donor and an intermediate π -acceptor. The imino nitrogen atoms are also weak σ -donors, but in general, the π -accepting properties of the imino nitrogen atoms are better when compared to the terpyridine nitrogen atoms [84, 93]. Due to the close similarities between both types of ligands, comparisons could be elaborated but with special caution as unique properties have been observed once the 2,6-bis(imino)pyridine compounds are coordinated to the metal [54].

In general terms, the compounds contain 1:1 metal to ligand ratio (figure 4.3) and three chloride ligands are completing the octahedral arrangement. RuL1 and RuL2 were characterized by a variety of techniques including elemental analysis, ESI-MS spectrometry, UV-Vis, IR, EPR and ¹H NMR spectroscopy. The elemental analyses were found in agreement with the proposed structures and stressed the purity of the samples. The compounds are scarcely soluble in water, ethanol and methanol, but they are highly soluble in polar organic solvents such as dmsO, dmf and slightly soluble in acetonitrile.

From IR studies, several changes were observed in the spectra of RuL1 and RuL2 when comparing with the corresponding free ligands spectra. Table 4.4 summarizes some selected IR peaks, the corresponding assignment and frequencies in the mid-IR region, confirming the presence of the ligand and coordinating to Ru. A sharp vibration peak assigned to the ν (Ru-Cl) stretching mode was observed in RuL1 at 325 cm⁻¹, and in RuL2 at 318 cm⁻¹; these values are also in accordance with the proposed structure [88, 90, 94].

For comparison reasons some IR bands present in $[\text{Ru}(\text{tpy})\text{Cl}_3]$ (tpy=2,2':6',2''-terpyridine) are also included. The C=N bond stretching frequency in $[\text{Ru}(\text{tpy})\text{Cl}_3]$ is present at higher values when comparing the values for RuL1 and RuL2. This effect could be attributed to the reduced backbonding effect in terpyridine [84, 95, 96]. Similarly, when comparing data of the Ru-Npy bond stretching frequency of $[\text{Ru}(\text{tpy})\text{Cl}_3]$, lower values are found than the values found for RuL1 and RuL2; this means also a reduced backbonding effect of terpyridine in comparison with L1 and L2.

So the IR spectra of RuL1 and RuL2, upon coordination are changed as follows: the strong HC=N(imino)bond stretching vibrations of the ligands is quite decreased in intensity, which is clearly associated to metal coordination. The sharp band at 1640 cm^{-1} assigned to the ν HC=N stretching mode of the imino moiety is shifted to lower frequency in RuL1 (1595.5 cm^{-1}) and comparable values are observed in case of RuL2. This shift supports the participation of the imino nitrogen in binding to the metal ion. Although small shifts are observed for the C=N(pyridine) bond stretching vibrations at lower frequency (RuL1 and RuL2), they are compatible with coordination. As expected, the changes are not so dramatic in the high-frequency region [78]. On the contrary the changes in the pyridine vibrations in the low frequency region are easily assigned for both coordination compounds. For instance, the rocking (ρ) pyridine vibrations (around 650 cm^{-1}), in the free ligands, are shifted to lower frequency ($75\text{-}35\text{ cm}^{-1}$) in the coordination compounds. The series of weak bands between 3100 and 2800 cm^{-1} are related to (C-H) modes of vibration. Also, some weak bands located between $2000\text{-}1750\text{ cm}^{-1}$ can be assigned to overtones of the aromatic rings. The bands appearing at 374.3 cm^{-1} for RuL1 and 390 cm^{-1} for RuL2 can be attributed to ν (M-N) bond vibration of the pyridine nitrogen-Ru atoms; the bands appearing around 600 cm^{-1} , can be assigned, to ν (M-N) bond vibration of the imino nitrogen-Ru atoms. Finally the strong peaks at 325 and 328 cm^{-1} are attributed to the Ru-Cl stretching bond vibration, values that are also comparable to other Ru(III) with chlorido-ligands in meridional conformation [97].

Table 4.4 IR assignment of the ligands L1 and L2 and RuL1 and RuL2 complexes. Selected peaks only.

Peaks	Frequencies (cm^{-1})				
	L1	RuL1	L2	RuL2	$[\text{Ru}(\text{tpy})\text{Cl}_3]$
ν (HC=N)	1640	1595.5	1636	1590	-
ν (C=N)pyridine	1565	1540	1587-1560	1550-1540	1595
ν (C=C)	1481-1451	1476-1440	1456-1445	1476-1457	1471-1387
ρ pyridine	642	606.8	668	593	644
ρ_{out} pyridine	505	452	526	474	432
aryl substitution	852-815	859-816	866-714	816-746	821-730
ν Ru-Npy	-	374.3	-	390	358
ν Ru-Nimino	-	607-586	-	593	-
ν Ru-Cl	-	325	-	328	310

The absorption spectra for the ligands and their complexes, in the UV-Vis region, were recorded using a Varian CARY 50 UV/VIS spectrophotometer operating at room temperature. Due to the poor solubility in water of RuL1 and RuL2, freshly prepared dmf solutions (0.148 mM and 0.136 mM) were analyzed by this technique. The spectra of RuL1 and RuL2 are characterized by intense peaks in the region that comprises 200-700 nm. The spectra in the visible region are dominated by the expected $d \rightarrow \pi^*$ MLCT bands and in the UV region by ligand-centred $\pi \rightarrow \pi^*$ transitions. The bands appearing at 317 nm ($\log \epsilon_M = 3.74$) and 390 nm ($\log \epsilon_M = 3.80$), for RuL1, and at 293 nm ($\log \epsilon_M = 3.78$) and 387 nm ($\log \epsilon_M = 3.72$), for RuL2, are considered mainly as intraligand charge-transfer transitions, as they have high molar absorption coefficients and have been observed in the free ligands as well (Figure 4.11). The energy of the $\pi \rightarrow \pi^*$ -transition in free L1 (at 300 nm and 356) is lower for RuL1 (at 317 nm and 390), which is consistent with coordination of L1 [97]. The same effect could be observed in case of the free L2 and RuL2. The transitions observed in the visible region in these compounds, are comparable to other Ru(III) complexes involving nitrogen donor molecules [87, 88, 97-99]. The lowest energy absorption bands at 482 and 509 nm for RuL1 and RuL2, respectively, are assigned to the spin-allowed $d\pi(\text{Ru(III)}) \rightarrow \pi^*(\text{L1 and L2})$ MLCT transition, with shoulders at 594 and 613 nm respectively.

The lowest energy $d\pi(\text{Ru(III)}) \rightarrow \pi^*(\text{L})$ band is observed for RuL2 at 509 nm. This red shift, when comparing to RuL1 band (482 nm), could be related to the presence of the electron-

releasing isopropyl moieties at *ortho* position of the aryl ring, directly interacting with the imino nitrogen atoms in L2.

For comparison, the λ_{\max} for the analogous compound $[\text{Ru}(\text{tpy})\text{Cl}_3]$ at 282($\log\epsilon_M=4.17$), 315($\log\epsilon_M=4.20$), 412($\log\epsilon_M=3.66$) and 482.7($\log\epsilon_M=3.33$) nm, are mentioned. Similar values to both RuL1 and RuL2 are observed, an indicator of the close similarity of the electronic nature of these Ru(III) compounds (spectra not included). The MLCT band maximum of $[\text{Ru}(\text{tpy})\text{Cl}_3]$ is located at almost the same wavelength than that of RuL1 and RuL2. This small difference can be explained by considering that the energy gap between electronic levels is almost unchanged between $[\text{Ru}(\text{tpy})\text{Cl}_3]$ and the RuL1 and RuL2 systems, despite the better π -acceptor properties of L1 and L2. A related effect in other Ru compounds has been reported for systems containing terpyridine- and benzimidazole-containing ligands [100].

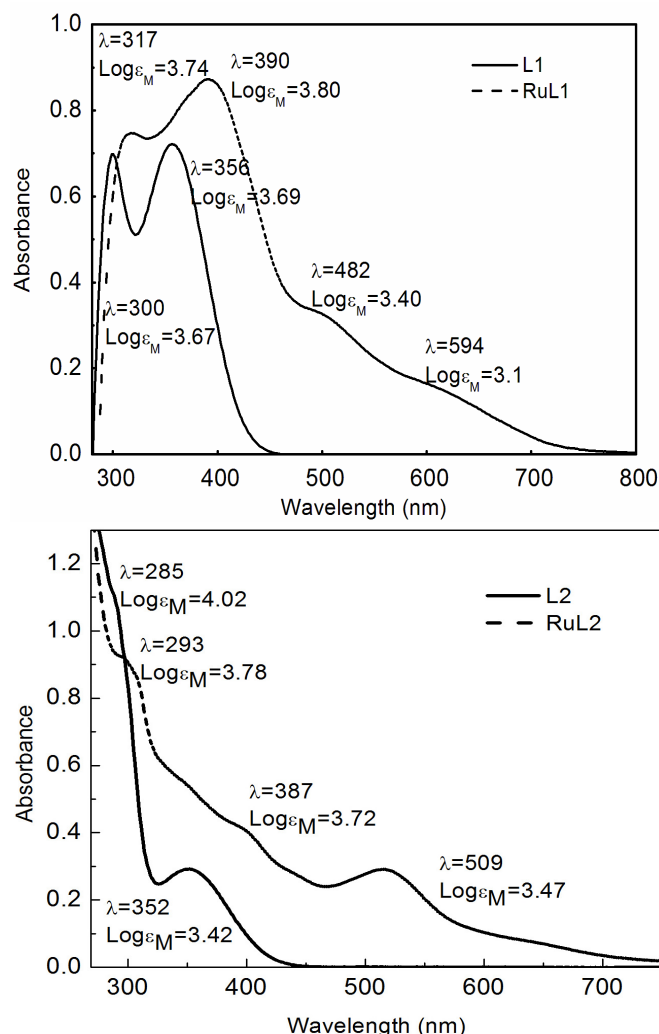


Figure 4.11 Absorption spectra of RuL1 and RuL2 in dmf along with their corresponding free ligands at 294 K.

The ESI-MS spectrum of RuL1 exhibits a positive peak at $m/z=582.07$ (calc, 582.44), which corresponds to the cationic structure, $[\text{Ru}(\text{C}_{25}\text{H}_{27}\text{N}_3)(\text{CH}_3\text{CN})\text{Cl}_2]^{1+}$. A mixture of $\text{CH}_3\text{CN}/\text{H}_2\text{O}$, 80:20 was used as eluent. The MS peak exhibits the correct isotopomer distribution as expected from the number of chlorine atoms and the Ru isotope distribution. In analogy, the ESI-mass spectrum of RuL2 exhibits one major positive peak at $m/z = 666.18$ (calc, 666.70) which corresponds to the structure $[\text{Ru}(\text{C}_{31}\text{H}_{39}\text{N}_3)(\text{CH}_3\text{CN})\text{Cl}_2]^{1+}$, in the same eluent; also this peak exhibit the correct isotopomer distribution.

Although RuL1 and RuL2 are paramagnetic, ^1H NMR spectroscopy can provide important structural information for such compounds [101, 102]. Figure 4.12 shows the ^1H NMR spectrum of RuL1 and the corresponding assignment of peaks. Due to its paramagnetic nature, the spectrum of RuL1 shows 6 paramagnetically shifted and broadened peaks that were assigned on the basis

of integration and proximity to the paramagnetic Ru centre; these peaks are distributed in a wide frequency range. Due to the symmetry in the complex, the protons forming part of the structure are magnetically equivalent in pairs, so only 6 resonances are observed in the spectrum. Striking similarities have been observed for paramagnetic compounds of Co and Fe with similar bis(imino)pyridine ligands [42, 45, 67]. The loss of multiplicity is attributed to broadening due to the proximity of the paramagnetic centre. The integration values are in agreement with the proposed structure (assignment data: $\delta=4.636$ (s, 4H, H₇, H_{7a}, H₉ and H_{9a}), 1.5983(s, 6H, 3H₁₂ and 3H_{12a}), -1.850 (broad s, 2H, H₂ and H_{2a}), -2.417(broad s, 12H, 3H₁₁, 3H_{11a}, 3H₁₃ and 3H_{13a}), -4.291(broad s, 1H, H₃) and -27.850 ppm (broad, 2H, H₄ and H_{4a})). The strong coordination of the aryl-substituted imine arm to the paramagnetic ruthenium centre is confirmed by the large upfield shift ($\delta=-27.850$ ppm) of the N=C-H resonance, as well as its broad linewidth. Particular attention should be directed to the resonance of the hydrogen atoms, H₁₁ and H₁₃, belonging to the methyl moieties in the aryl group, as they present a high field shift and display a very broad linewidth, suggesting that this aromatic ring is spatially very close to the paramagnetic ruthenium centre. The presence of just one signal for the methyl group protons located at the *ortho* position in the aryl ring suggests a free rotation about the N-C axis. The very clean spectrum indicates a high purity of the sample. No relevant change in the spectrum was found after several hours at 298 K. Only, after 9 days a partial reduction and probably coordination of solvent is observed. The powder EPR of the solid RuL1 just shows a single very broad, uninformative line centred at $g = 2.10$

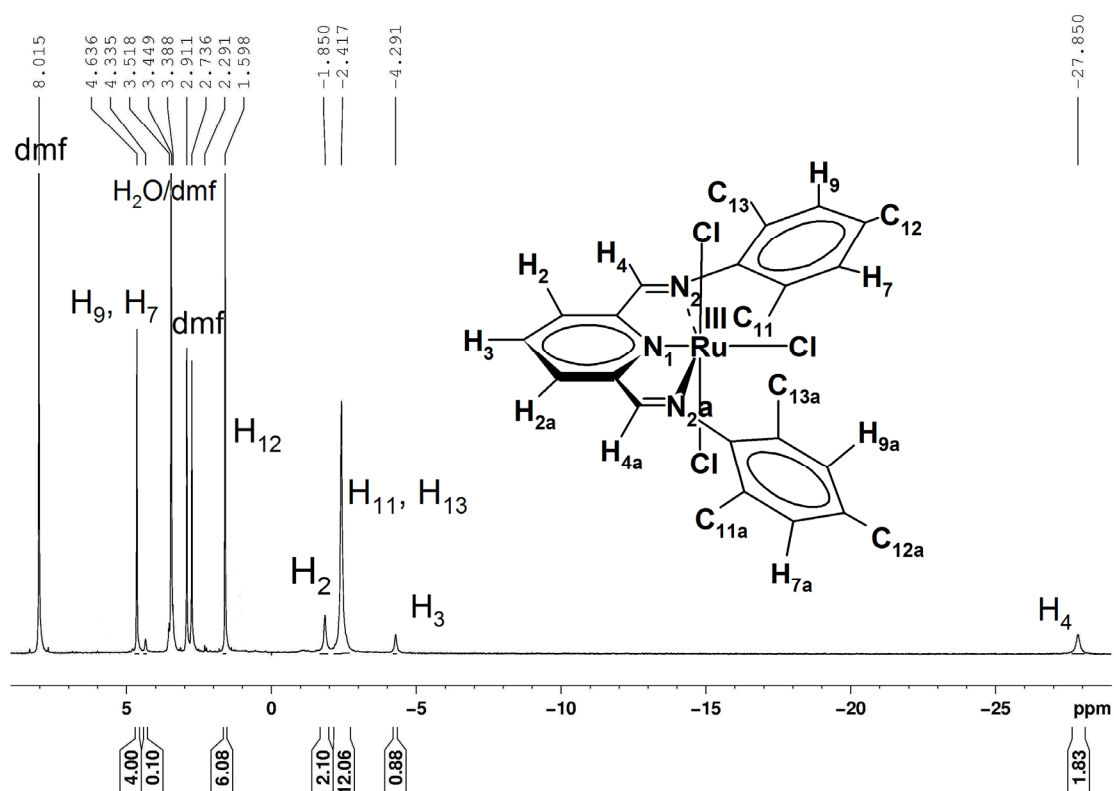


Figure 4.12 ^1H NMR spectrum of the paramagnetic compound, RuL1, and corresponding assignment recorded in deuterated dmf at 294 K. For clarity reasons, in the schematic representation, the hydrogen atoms belonging to the methyl groups are not depicted. A trace of water is visible at 3.38 ppm.

Closely comparable results were obtained in case of the paramagnetic RuL2 as observed in Figure 4.13, which shows the ^1H NMR spectrum of RuL2 and the corresponding peaks assignment. The spectrum of the paramagnetic RuL2 shows 7 paramagnetically shifted and broadened peaks that were assigned, on the basis of integration and proximity to the paramagnetic Ru centre, and which are distributed in the range from 6 to -29 ppm. Due to the symmetry in the complex, the protons forming part of the structure are magnetically equivalent in pairs, so only 7 resonances are observed in the spectrum. The integration values are in agreement with the proposed structure (assignment data: $\delta=4.93$ (s, 4H, H₉, H₁₁, H₂₂ and H₂₄), 0.57(s, 2H, H₁₀ and H₂₃), -1.24 (broad s, 24H, 3H₁₄, 3H₁₅, 3H₁₇, 3H₁₈, 3H₂₇, 3H₂₈, 3H₃₀ and 3H₃₁), -1.90(broad s, 2H, H₂, and H₄), -4.25(broad s, 1H, H₃), -6.40(broad s, 4H, H₁₃, H₁₆, H₂₆ and H₂₉),

and -28.53 ppm (broad, 2H, H₆ and H₁₉). Again, coordination of L2 to the metal centre, through the imino nitrogen, is confirmed by the large upfield shift ($\delta = -28.53$ ppm) of the N=C-H resonance peak as well as its broad linewidth. The isopropyl moieties in the aryl rings are also affected by the paramagnetic nature of Ru(III) as they show a high field shift, which probes also their magnetic equivalence. The same effect could be detected in case of the resonance peaks of the hydrogen atoms in the pyridine ring, which probes that coordination of L2 is taking part. Important to mention is the subtle influence of the electron-releasing isopropyl groups that generates, higher upfield shift of the resonance peak assigned to the imino function (H₆, H₁₉) when comparing with the equivalent resonance peak in RuL1 (H₄). The powder EPR of the solid RuL2 just shows a single very broad, uninformative line centred on $g = 2.05$.

The very clean NMR spectrum indicates a high purity of the sample. No relevant change in the spectrum was found after several hours at 298 K. Only, after 5 days a partial reduction and probably coordination of solvent is observed.

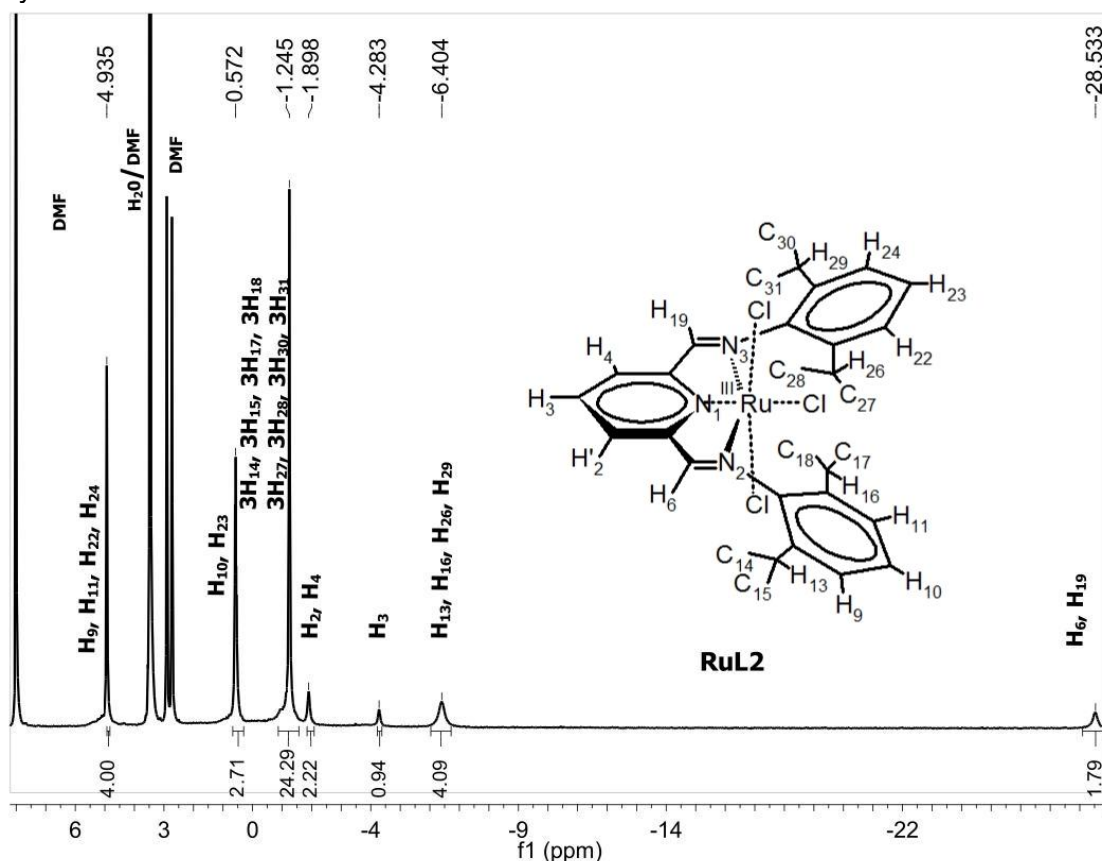


Figure 4.13 ¹H NMR spectrum of the paramagnetic compound, RuL2, and corresponding assignment, recorded in deuterated dmf at 294 K. In the schematic representation, the hydrogen atoms belonging to the isopropyl groups have been omitted for clarity. A trace of water is visible at 3.38 ppm.

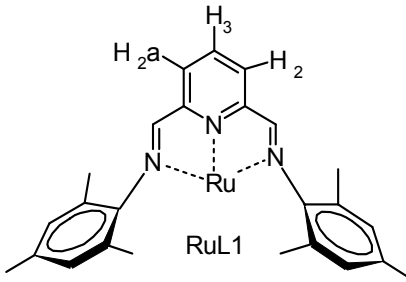
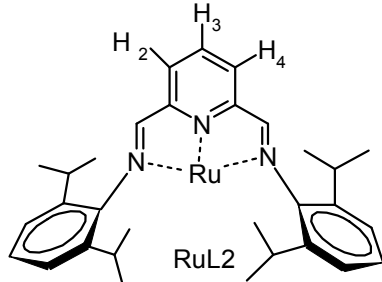
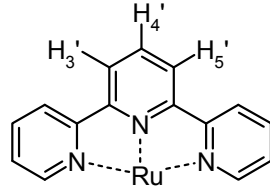
The proton resonance peaks of the hydrogen atoms localized in the pyridine central moiety in [Ru(tpy)Cl₃] are differently affected by the influence of the paramagnetic metal centre as observed from the magnetic shifts. While the *para* hydrogen atom in the central pyridine in tpy is substantially affected by coordination to the paramagnetic Ru(III) (-23.188 ppm), the hydrogen atoms at the *meta* positions are less affected (5.455 ppm). When comparing with the paramagnetic influence generated in RuL1 and RuL2, it is clear that, reduced paramagnetic effect is observed in the hydrogen at *para* position in the pyridine moiety while higher effect is observed in the hydrogen atoms in *meta* position. This effect could be attributed to the increased π -accepting ability of the imino moieties in L1 and L2 once coordinated to Ru, in comparison with the pyridine moieties in 2,2':6',2''-terpyridine (Table 4.5).

Even though single crystals of the Ru(III) compounds described above have not been obtained and therefore the structures of the compounds cannot be given in detail, the conclusions reached upon application of the spectroscopic techniques, strongly suggest that coordination of L1 and L2 takes place in a near-octahedral meridional geometry through the pyridyl and imino-

Chapter 4

nitrogen atoms in a tridentate mode with three chloride ligands completing the octahedral coordination.

Table 4.5 Selected ^1H NMR shifts(ppm) of the Ru(III) compounds, RuL1, RuL2 and $[\text{Ru}(\text{tpy})\text{Cl}_3]$ in deuterated dmf at 294 K. In the schematic representation, the chloride ligands have been omitted for clarity.

		
$\text{H}_2, \text{H}_{2a}: -1.850 \text{ ppm}$ $\text{H}_3: -4.291$	$\text{H}_2, \text{H}_4: -1.898 \text{ ppm}$ $\text{H}_3: -4.382$	$\text{H}_3', \text{H}_5': 5.455 \text{ ppm}$ $\text{H}_4': -23.188$

4.3.3 DNA model base interaction

Although the mechanism of action of the cytotoxic Ru compounds is not yet elucidated in detail, a direct interaction with DNA is a likely possibility, among other mechanisms [17, 38, 103-106]. In order to shed some light on the coordination interactions between the ruthenium compounds studied in this project and DNA, the reaction with the model base 9-ethylguanine (9EtGua) was studied in detail. Even though this model reaction does not mimic the real interaction with DNA in the cells, it provides useful information on the reactivity of the complex, leaving-group liability and structural characteristics of the adduct formed. Furthermore, the ruthenium-nucleobase model complex formed could be a useful reference compound for the identification of analogous guanine adducts in the cells.

The experimental procedure followed for the synthesis of RuL1-2(9EtGua) was similar to the procedure describe for the synthesis of a closely related Ru compound ($[\text{Ru}(\text{tpy})(9\text{EtGua})(\text{H}_2\text{O})](\text{PF}_6)_2$) synthesized by van Vliet [39]. The reduction of Ru(III) takes part without any familiar reducing agent, reactivity that has been observed in other cases [39, 97]. It appears that ethanol may serve as the reducing agent and the coordination of the nitrogen-donor model base must favour even more the reduction process as the donor properties tend to stabilize the Ru(II)-oxidation number. The compound aquobis(9-ethylguanine)(2,6-bis(2,4,6-trimethylphenyl)iminomethyl)pyridine)ruthenium(II) perchlorate, abbreviated as RuL1-2(9EtGua), was prepared, in good yields, by treatment of RuL1 with 3 equivalents of 9EtGua in ethanol: water (see Experimental Section) as shown in figure 4.14. The compound was characterized by a variety of techniques including elemental analysis, ESI-MS spectrometry, UV-Vis, IR and ^1H NMR spectroscopy. In addition, RuL1-2(9EtGua) was studied by single-crystal X-ray diffraction.

Several experimental conditions were applied to force the coordination of 9EtGua to RuL2. Despite some chemical evidence (^1H NMR and UV-vis spectra, not shown) was suggesting the transformation of the starting materials, all attempts for the isolation of solid products remained unsuccessful. The reduced reactivity of RuL2 could be the result of steric factors, such as the bulky isopropyl substituents at *ortho* position in the phenyl moieties, which can protect the metal centre from further coordination. Further studies are needed to understand these steric effects.

The elemental analysis of RuL1-2(9EtGua) corresponds with a reduction of Ru(III) and coordination of 2 molecules of 9EtGua and one molecule of water to Ru(II). The IR spectrum further confirms the presence of 9EtGua and water coordinated to the structure (see table 4.6, selected peaks only). The most important evidence is the disappearance of the stretching Ru-Cl vibration peak, once a water molecule is coordinated to the metal, replacing the chloride ligand. The presence of the symmetric deformation H-OH bond vibration around 1560 cm^{-1} confirms the presence of water coordinated [78]. Most of the vibration peaks present a shift which could be interpreted as a result of coordination of 9EtGua and stabilization of the Ru(II)-oxidation state. The presence of perchlorate as counterion is evidenced by a strong and broad band near 1080 cm^{-1} and a sharp band near 620 cm^{-1} in the spectra of this compound that obscure other vibration peaks.

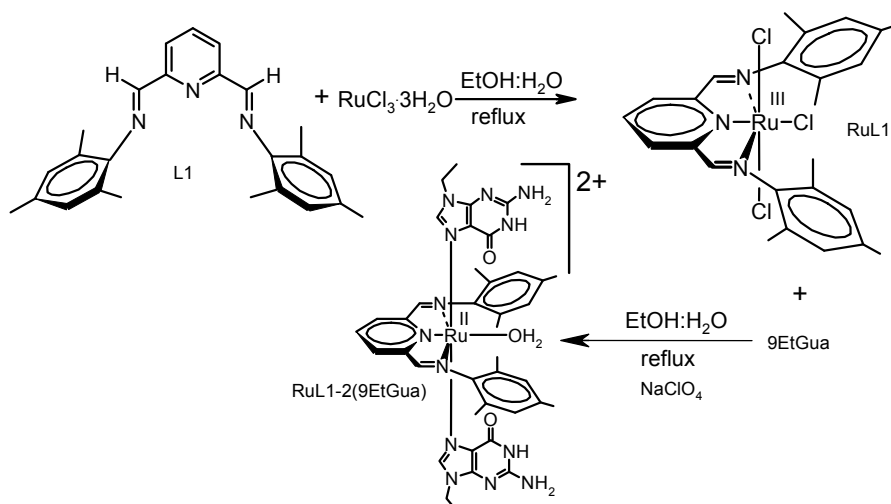


Figure 4.14 Schematic representation of the synthesis of RuL1-2(9EtGua).

Table 4.6 Characteristic IR bands (4000-300) and assignments for RuL1 and RuL1-2(9EtGua). Selected peaks only.

Peaks	Frequencies	
	RuL1	RuL1-2(9EtGua)
ν (HC=N)	1595.5	1603.5
ν (C=N)pyridine	1540	1578-1558
ν (C=C)	1476-1440	1506-1460
ρ pyridine	606.8	Counterion overlapped
ρ_{out} pyridine	452	397
ν Ru-Npy	374.3	374
ν Ru-Nimino	607-586	Counterion overlapped
ν Ru-Cl	325	-
ν_{s} (H-OH)	3200	3300-3200
δ_{s} (H-OH)	1595.5	1568 coordinated
ν_{s} (O-ClO ₃ ⁻)	-	1081.5
		622

The ESI-MS spectrum of RuL1-2(9EtGua) exhibits four main positive peaks, all them confirming the presence of the proposed compound and with similar pattern than the analogous compound [Ru(tpy)(9EtGua)₂(H₂O)](PF₆)₂·3H₂O [39] mass spectrum. The MS peaks exhibit the correct isotopomer distribution mainly derived from a single Ru atom.

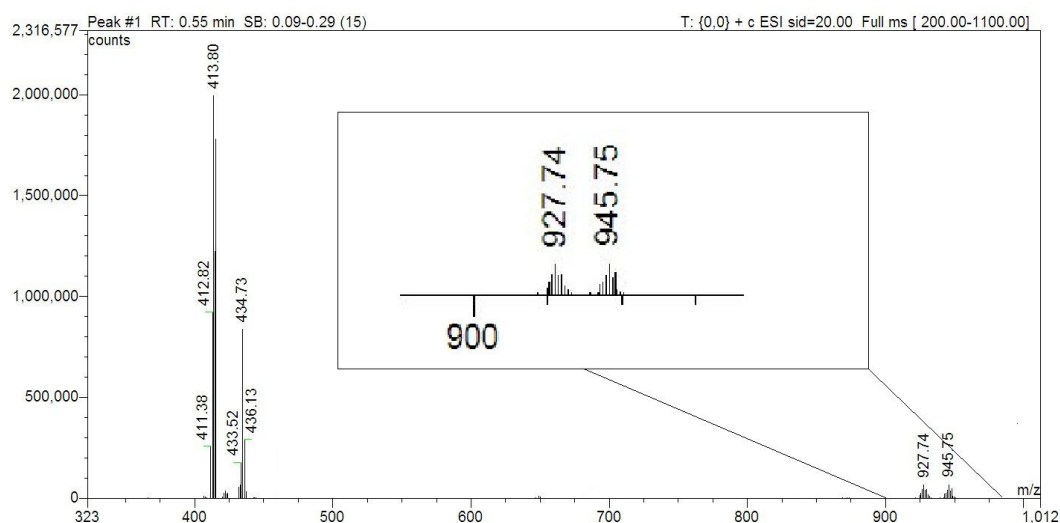


Figure 4.15 ESI-MS positive ion spectrum from RuL1-2(9EtGua) (m/z in Da). See experimental section for calculated data. Magnified details of selected fragments are shown in the inset.

The electronic spectrum of RuL1-2(9EtGua) shows broad and intense visible bands between 400 and 600 nm due to MLCT transitions (figure 4.16). The MLCT bands located at 477 and 552 nm, in case of RuL1-2(9EtGua) resembles the typical MLCT bands of a Ru(II)-tpy

coordination compound [92, 98, 99, 107, 108], which is a good indicator of the similar electronic nature of these compounds. In addition, intense peaks by ligand-centred $\pi \rightarrow \pi^*$ -transitions are present in the UV region.

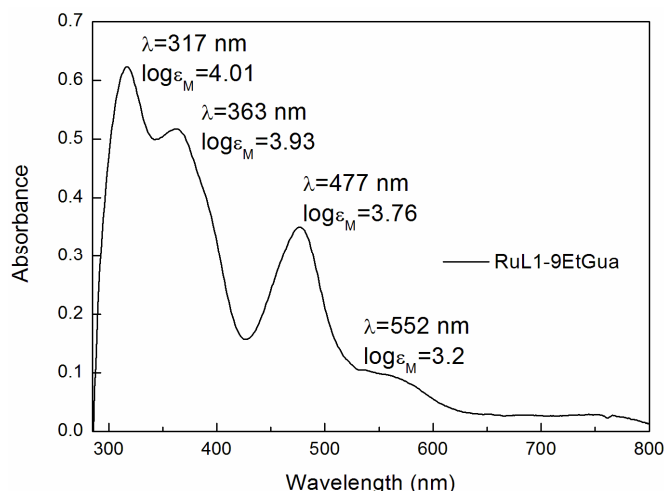


Figure 4.16 Absorption spectrum of RuL1-2(9EtGua) in methanol at 294 K.

The synthesis, stability and isolation of RuL1-2(9EtGua) as a monoquo compound are favoured by the intramolecular hydrogen-bonding properties of the 9EtGua molecules. The compound and ligands display resolved ^1H NMR spectra in deuterated methanol, thereby providing important structural evidence. Figure 4.17 shows the ^1H NMR spectrum of RuL1-2(9EtGua), along with the free 9EtGua spectrum and the corresponding assignments, which were confirmed by two-dimensional NMR studies. The presence of just a few peaks suggests a high symmetry in the system. The frequency ranges where the resonance peaks are observed demonstrate the diamagnetic nature of this compound. The integration values are in agreement with the proposed structure. The very clean spectrum indicates a high purity of the sample. No relevant change in the spectrum was found after several days.

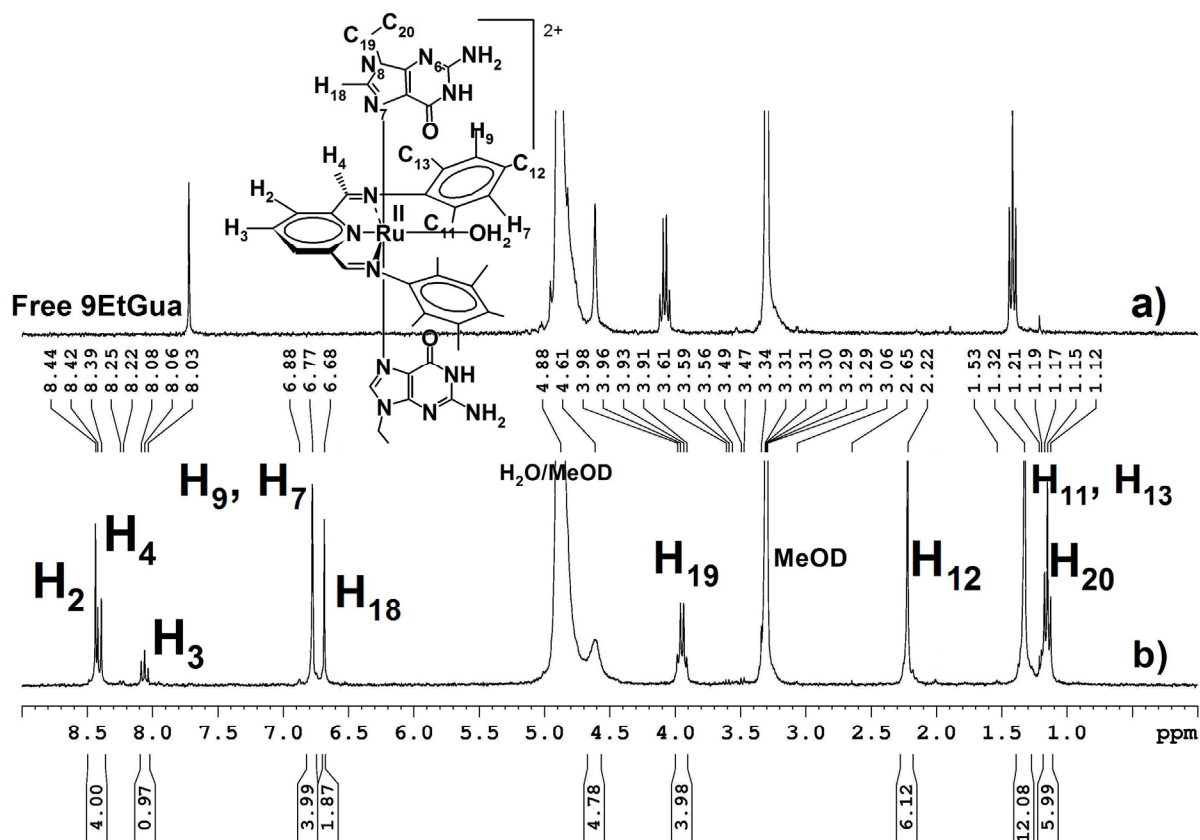


Figure 4.17 ^1H NMR spectrum of free 9EtGua (a) and RuL1-2(9EtGua) (b) in deuterated methanol at 294 K.

Overall, the ^1H NMR spectrum of this diamagnetic RuL1-2(9EtGua) compound displays the same pattern of resonances present in the free L1 (see Experimental section). The presence of one signal for the methyl groups, H_{11} and H_{13} is consistent with its high symmetry and the presence of a hindered rotation of the aryl ring about the N-C axis, were also observed in related compounds of cobalt and iron [70].

The influence of the temperature was recorded in a methanolic solution of RuL1-2(9EtGua) (figure 4.18). At room temperature (298 K) and at low temperature (218 K), the ^1H NMR spectra of RuL1-2(9EtGua) are very similar, showing just a slight shift of the resonance peaks corresponding to protons H_9 or H_7 and H_{18} , and the originally broad peak assigned to the amino group in 9EtGua (4.61 ppm) shows a well-resolved resonance at low temperature. From all the information just mentioned, it is clear that in the case of RuL1, two model 9-ethylguanine (9Etgua) bases are coordinated to the structure in *trans* configuration, through N7.

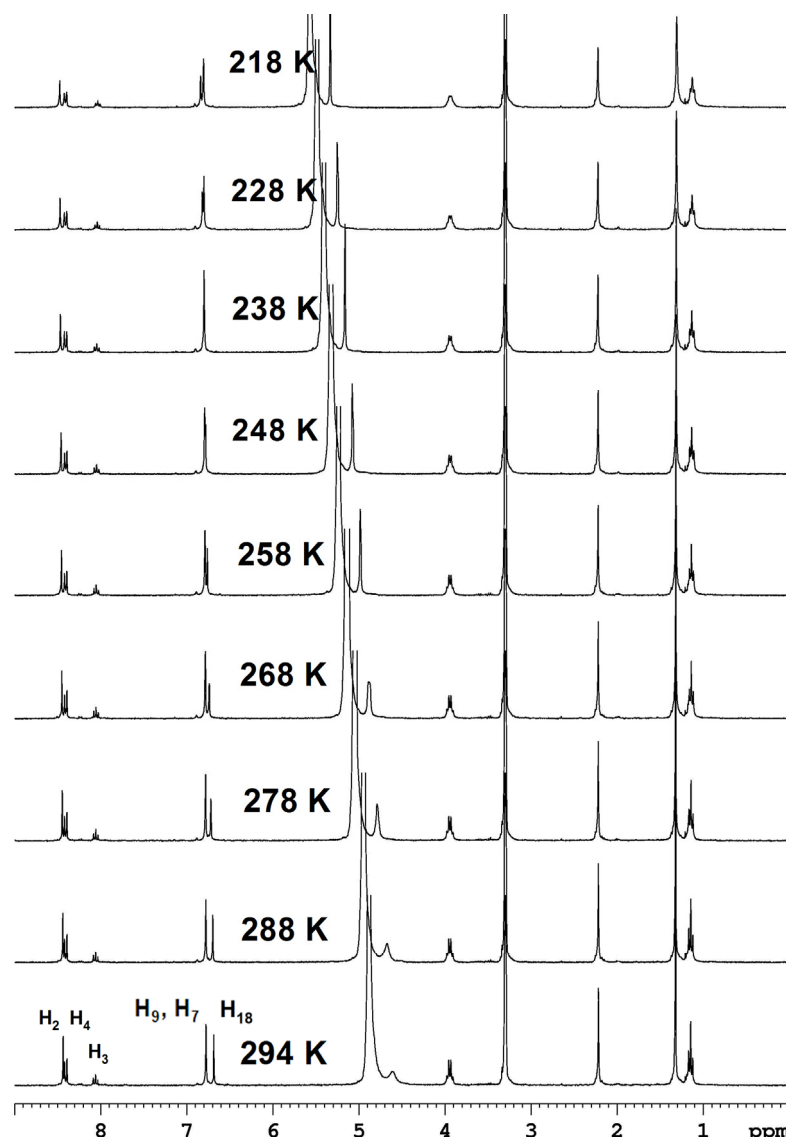


Figure 4.18 Variable temperature 1D ^1H NMR spectra of RuL1-2(9EtGua) in a temperature range from 218-294K recorded in deuterated methanol.

Crystals of RuL1-2(9EtGua) suitable for X-ray diffraction studies were grown from a concentrated methanol solution. One dark brown block crystal was mounted on a glass fibre. In the structure of RuL1-2(9EtGua) (*Fdd2*, $Z = 8$), the asymmetric unit contains one half of the Ru compound, because it is located at sites of twofold symmetry, one counter anion, ClO_4^- , and one lattice methanol molecule. The structure of RuL1-2(9EtGua) is ordered and its complex cation unit is shown in Figure 4.19 and all crystallographic data are listed in table 4.7. Table 4.8 includes selected bond distances and angles for RuL1-2(9EtGua). These results confirm not only the

chemical structure of RuL1-2(9EtGua), initially described by the previous evidence, but also confirm the chemical structure of RuL1, the starting material.

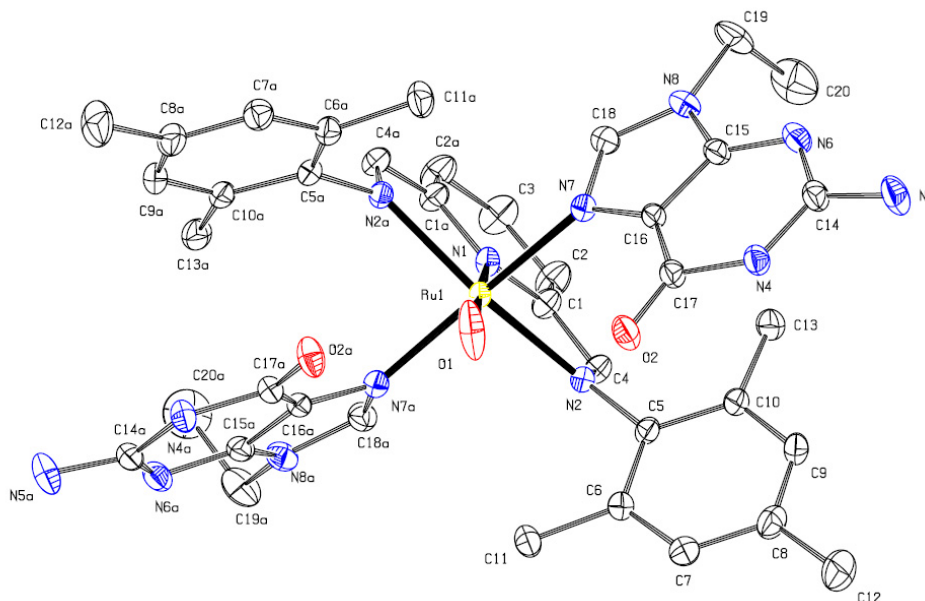


Figure 4.19 Displacement ellipsoid plot (50 % probability level) of the asymmetric unit at 150 K. Half of the compound is symmetry generated via twofold symmetry (the twofold axis runs through the N1 and C3 atoms). For clarity reasons, the ClO_4^- counter anion, the lattice methanol molecule and the H-atoms are not depicted.

In RuL1-2(9EtGua), the immediate Ru coordination sphere is a distorted octahedron, with the major distortion arising via the N2-Ru1-N2a angle, at $156.06(7)^\circ$, which is remarkable similar to the behaviour observed in Ru(II)-terpyridine systems [88]. This angle is considerably smaller than the ideal angle of 180° and the same effect in related Ru(II) compounds is already reported in literature [83, 84]. The Ru1-N1 (pyridyl) bond ($1.928(2) \text{ \AA}$) is shorter than the Ru1-N2 (imino) bond ($2.1221(13) \text{ \AA}$). This shortening could be present to optimize the chelation of L1, as observed in case of coordination of tpy where the central metal-Npyridine bond shortens while the terminal ones lengthen, which maintain the typical tpy bite angle around 79 degrees [88, 90]. For RuL1-2(9EtGua), the bite angle is $78.03(4)$ degrees.

Table 4.7 Crystallographic data for RuL1-2(9EtGua).

Abbreviation:	RuL1-2(9EtGua)
empirical formula	$\text{C}_{39}\text{H}_{47}\text{N}_{13}\text{O}_3\text{Ru} \cdot (\text{MeOH})_2(\text{ClO}_4)_2$
Fw	1109.95
crystal symmetry	orthorhombic
Space group	<i>Fdd2</i> (No. 43)
<i>a</i> , \AA	25.2350(1)
<i>b</i> , \AA	30.8420(2)
<i>c</i> , \AA	12.2446(1)
β ($^\circ$)	90
<i>V</i> , \AA^3	9529.95 (11)
<i>Z</i>	8
<i>T</i> , K	150(2)
ρ_{calcd} , g/cm^3	1.547
μ , mm^{-1}	0.52
<i>R</i> 1 ^a	0.019
<i>wR</i> 2 ^b	0.048
GOF	1.06
$\Delta\rho_{\text{max}}$, e \AA^{-3}	0.30
$\Delta\rho_{\text{min}}$, e \AA^{-3}	-0.30
Flack parameter	-0.025 (14)

^a $R1 = \sum ||F_o| - |F_c|| / \sum |F_o|$. ^b $wR2 = \{\sum [w(F_o^2 - F_c^2)^2] / \sum [w(F_o^2)^2]\}^{1/2}$

The double bond character of the imino linkage C4-N2 is retained ($1.299(2) \text{ \AA}$, while for L1 is $1.2494(17) \text{ \AA}$, see appendix A) although the difference with respect to the aromatic double bond distance (C1-N1, $1.3612(19) \text{ \AA}$) is smaller than the difference observed in the free ligand. Another

important change is the reduction in the C1-C4 bond distance. It is noticeable that the planes of the substituted-phenyl rings are oriented essentially orthogonal to the plane of the backbone (76.41°) as observed in other iron, cobalt and ruthenium related systems [67, 84]. The *ortho*-methyl substituents in the phenyl rings are not bulky enough to protect the metal centre as observed in other bulkier substituents as isopropyl [67]. The angle N1-Ru1-O1 is normal for an octahedral conformation (180.00(2)°).

Table 4.8 Selected geometric parameters (Angstroms, degrees) for RuL1-2(9EtGua).

Distances (Angstroms)			
Ru1-N1	1.928(2)	C5-N2	1.441(2)
Ru1-N2	2.1221(12)	C1-C4	1.440(2)
Ru1-N7	2.0990(12)	C1-C2	1.392(2)
Ru1-O1	2.084(2)	C5-C10	1.410(2)
C1-N1	1.3612(19)	N7-C18	1.319(2)
C4-N2	1.299(2)	N8-C18	1.356(2)
Angles (Degrees)			
N1-Ru1-O1	180.00(2)	C4-N2-C5	116.09(13)
O1-Ru1-N2	101.97(4)	N1-C1-C2	120.74(16)
O1-Ru1-N7	87.92(4)	N1-C1-C4	111.62(15)
N1-Ru1-N2	78.03(4)	O2-C17-N4	118.00(15)
N1-Ru1-N7	92.08(4)	N2-C4-C1	118.04(14)
N2-Ru1-N7	85.13(5)	N2-C5-C6	119.75(13)
C1-N1-C1a	119.87(19)	C5-C6-C11	121.10(14)

The Ru1-N7 bond distance, 2.0990(12)Å, is slightly shorter when comparable with related structures [109], where the reported Ru-N7 bond distances are found between 2.122 and 2.131 Å. Worth mentioning is that this Ru1-N7 bond distance is intermediate between the values found for the Ru-pyridyl bond (Ru1-N1, 1.928(2) Å) and the Ru-imino bond (Ru1-N2, 2.122(12) Å). The keto group belonging to the 9EtGua moiety is oriented to the centre of the phenyl rings and slightly bent out of the plane with the O2-C17-C16-C15 torsion angle of 175.71(16)°. It is also important to stress the fact that the 9EtGua moieties are twisted by 38.53° from the plane describe by Ru1-O1 (torsion angle, O1-Ru1-N7-C16, 38.52(13)°). The relative orientation of the two 9EtGua molecules is classified as head-to-tail. This energetically less favoured orientation could be related to the extra stabilization generated by hydrogen bonds D-H...A between the protons belonging to the water molecule coordinated and the oxygen from keto groups in 9EtGua (O1-H1...O2, O1...O2 = 2.5436(14) Å).

4.3.4 Cytotoxic activity studies

Despite of the large amount of research developed in the study of Ru-anticancer compounds and, moreover, the introduction of two Ru(III)-compounds in clinical trials, the biological mechanism of action of ruthenium complexes is still largely unknown [19].

The most cited hypothesis states that given the kinetically inertness of the Ru(III) coordination compounds in comparison with the corresponding Ru(II) analogues, an “activation by reduction” mechanism must be involved in the biological activity of some Ru-compounds [2, 10, 110, 111], although direct interaction with DNA or other biological mechanisms could not be totally discharged [112].

As part of the studies required for the understanding of the principles involved in the biological activity of this group of Ru(III) potential anticancer compounds, the determination of the cytotoxicity represents, nowadays, a controversial topic. It has been demonstrated that NAMI-A and KP1019, the most promising anticancer Ru(III) compounds have remarkable different anticancer properties. While NAMI-A is found to be unable to generate an acute cytotoxic effect (IC₅₀>100µM), it does inhibit metastasis formation and growth [106, 113] in mouse models. In contrast, KP1019 develops a moderate cytotoxicity against selected human tumour cell lines [114].

This peculiar biological behaviour of NAMI-A, that comprises inactivity towards primary tumours and remarkable activity towards secondary metastasis tumours has stressed the need of more effective assays for the identification of potential Ru-anticancer compounds. In view of this information, Dyson *et al.* [103] concluded that the dominance of the IC₅₀ values as a first screen

Chapter 4

for a putative drug should be treated with caution and moreover, the selection of the appropriate cells targets must become the first task in the study of the Ru-biological activity.

With this conceptual frame, the *in vitro* cytotoxicity data (IC₅₀) of some reported Ru(III) compounds against different tumour cell lines are summarized in table 4.9.

It is evident from these data that several incubation conditions and cell lines have been used in order to estimate the cytotoxic activity which makes more difficult any comparison or visualization of a structure activity relationship. Worth mentioning the fact that for most of the compounds, the cytotoxicity is rather moderate. Major efforts have been directed in the study of a structure activity relationship for NAMI-A, KP1019 and chemically related compounds [114-117]. Recent investigations on the antiproliferative activity for KP1019 and related derivatives, concluded that differences in the cytotoxic activity correlate with the reduction potentials largely, though not perfectly, which means that other physicochemical properties might be involved [115, 116].

To obtain further biologically relevant information on Ru(III) compounds, the free ligands L1-L4, and the compounds RuL1 and RuL2 were evaluated for their capability of inhibiting tumour cell growth *in vitro*, using seven human cell lines, i.e. A498, EVSA-T, H226, IGROV, M19, MCF-7 and WIDR. Cisplatin and doxorubicin were used as reference cytotoxic compounds. The resulting cytotoxic activity (expresses as IC₅₀ values) obtained after continuous exposure of the cells to the compounds for 120 h is concentrated in table 4.10. The IC₅₀ value represents the minimal amount of drug needed to inhibit 50% of the cancer cell growth.

On the basis of these results, most of the compounds tested show lower cytotoxic effects than cisplatin, but all compounds present IC₅₀ values within the micromolar range. This is generally considered as a moderate cytotoxic activity. The only exceptions were 2,2':6',2"-terpyridine and RuL2 which present higher cytotoxic effect than cisplatin. The presence of cytotoxic activity by itself probes that all tested compounds are able to travel inside the cells.

Table 4.9 *In vitro* cytotoxicity assay (IC₅₀ values) of several Ru(III)-compounds from the literature.

Compound	L1210 ^a	HT29 ^a	SK-BR-3 ^a	SW480 ^a	CH1 ^a	S180 ^a	HeLa ^a
[Ru(tpy)Cl ₃] ^p	8±2						
Cisplatin ^b	1.3±0.4						
(H ₂ im)[<i>trans</i> -Ru(III)Cl ₄ (Him)(S-dmsO)], NAMI-A ^c		339±68	472±25				
(H ₂ ind)[<i>trans</i> -Ru(III)Cl ₄ (Hind)(S-dmsO)] ^c		212±22	169±10				
(H ₂ trz)[<i>trans</i> -Ru(III)Cl ₄ (Htrz)(S-dmsO)] ^c		322±32	415±48				
(Hatrz)[<i>trans</i> -Ru(III)Cl ₄ (atrz)(S-dmsO)] ^c		621±5	>1000				
(Hmtrz)[<i>trans</i> -Ru(III)Cl ₄ (mtrz)(S-dmsO)] ^c		315±22	517±70				
(H ₂ im)[<i>trans</i> -Ru(III)Cl ₄ (Him) ₂] ^d				840			
(H ₂ trz)[<i>cis</i> -Ru(III)Cl ₄ (Htrz) ₂]·2H ₂ O ^e		181±21.5	205±27	164±5			
(H ₂ trz)[<i>trans</i> -Ru(III)Cl ₄ (Htrz) ₂] ^e		127±4.5	169±20	113±8			
(H ₂ ind)[<i>trans</i> -Ru(III)Cl ₄ (Hind) ₂], KP1019 ^f				63±3	66±4		
(H ₂ ind) ₃ [Ru(III)Cl ₆] ^g				187±23	103±13		
(H ₂ ind) ₂ [<i>trans</i> -Ru(III)Cl ₅ (Hind)] ^g				37±2	35±2		
[Ru(III)Cl ₃ (ind) ₃] ^g				2.6±0.1	2.5±0.3		
[Ru(III)Cl ₂ (ind) ₄]Cl ^g				0.69	0.67		
<i>cis</i> -[RuCl ₂ (NH ₃) ₄]Cl ^h						63	
<i>cis</i> -K[Ru(eddp)Cl ₂]·3H ₂ O		30.3 ⁱ					30.3 ^j

^a L1210 Cisplatin sensitive mouse leukemia cell line; HT29 human colon carcinoma cell line; SK-BR-3 human mammary carcinoma cell line; SW480 human colon carcinoma cell line; CH1 human ovarian cell line; S180 murine tumour line; HeLa human cervical cancer cell line. ^b Results reported by van Vliet [39]. Incubation time=72h. tpy: 2,2':6',2"-terpyridine. ^c Results reported by Groessl [116]. Incubation time=96h. Him: 1H-imidazole, dmsO: dimethyl sulfoxide, Hind: 1H-indazole, Htrz: 1H-1,2,4-triazole, Hatrz: 4-amino-1,2,4-triazole, Hmtrz: 1-methyl-1,2,4-triazole. ^d Results reported by Arion [117]. Incubation time=24h. ^e Results reported by Arion [117]. Incubation time=96h. Htrz: 1H-1,2,4-triazole. ^f Results reported by Reisner [115]. Incubation time=96h. Hind: 1H-indazole. ^g Results reported by Jakupec [115]. Incubation time=96h. ^h Results reported by Menezes [118]. Incubation time=24h. ⁱ Results reported by Grguric-Sipka [119]. Incubation time=96h. eddpH₂: ethylenediamine-*N,N'*-di-3-propionic acid. ^j Results reported by Grguric-Sipka [119]. Incubation time=72h, IC₆₈

Chapter 4

Table 4.10 *In vitro* cytotoxicity assay of compounds synthesized incubated during 120 h.

Compound	Cell line ^a , IC ₅₀ (μM)						
	A498	EVSA-T	H226	IGROV	M19	MCF-7	WIDR
L1	93.7	23.9	36.3	82.8	57.9	15.0	59.5
L2	107.9	74.4	79.5	137.8	83.8	69.5	1000
L3	85.1	27.3	38.7	75.3	34.5	41.7	2.3
L4	80.9	12.3	20.0	36.0	19.3	24.4	3.9
tpy	0.38	0.23	0.25	0.57	0.47	0.23	0.29
RuL1	15.1	11.2	15.2	12.2	12.2	17.1	14.5
RuL2	4.1	4.0	4.3	4.1	3.9	4.3	4.1
[Ru(tpy)Cl ₃]	79.6	67.0	63.7	90.1	68.5	64.0	79.0
cisplatin	7.51	1.41	10.9	0.56	1.86	2.33	3.22
DOX	0.16	0.015	0.37	0.11	0.03	0.02	0.02

^a A498 Human renal carcinoma cell line; EVSA-T Human breast cancer cell line; H226 Human non-small cell lung carcinoma cell line; IGROV Human ovarian carcinoma cell line; M19 Human melanoma carcinoma cell line; MCF-7 Human breast adenocarcinoma cell line; WIDR Human colon adenocarcinoma cell line.

The cytotoxicity data (IC₅₀) of the free ligands (L1-L4) indicate that they are not potent cytotoxic agents; however, some interesting cytotoxicity trends were noted. First of all the cytotoxic activity data suggest a correlation with the bulkiness of the aryl moiety. L2 with the isopropyl radicals in *ortho* position of the aryl moiety presents the poorest cytotoxic effect. By the contrary the lesser bulky ligands, L1, L3 and L4 show a better cytotoxic activity. The presence of an electron donating methyl group in *para* position of the aryl moiety appears to have a limited influence on the cytotoxicity of the ligands, as only better IC₅₀ value for L3 in comparison with L4 (any methyl group) could be detected in the colon adenocarcinoma cell line, WIDR. The potent cytotoxic properties of L3 and L4 in this cell line stress the need of further studies for this family of bis(arylimino)pyridine compounds.

The Ru(III) compounds of both ligands, L1 and L2, show a remarkable cytotoxicity profile. Comparison between the cytotoxic activity of the free ligands and coordination compounds demonstrate that in both cases, the biological response is higher for the coordination compound so the metal has an important influence in the biological activity. In general terms, RuL1 (with IC₅₀ values ranging from 11.20-17.10 μM) is around four times more active than L1 while RuL2 (with IC₅₀ values ranging from 3.9-4.3 μM) is up to 33 times more active than the corresponding ligand in certain cell lines. The most dramatic effect is observed in the WIDR cell line, where L2 is found hardly active, while RuL2 present a potent toxic effect comparable to the cytotoxicity developed by cisplatin in the same cell line. Only in the MCF-7 (breast cancer) cell line ((ER)+(PgR)+), coordination of L1 has a negative impact.

Due to the close structural similarities between RuL1 or RuL2 and [Ru(tpy)Cl₃], the cytotoxic effect of this last compound was evaluated for comparison reasons. The fact that the free ligand (tpy) is much more active than the Ru compound is the most notorious difference. It is also important to notice that in general terms, RuL1 and RuL2 show better cytotoxic effect than [Ru(tpy)Cl₃] even though all three of them show, in general, remarkably potent cytotoxic activity than previously reported Ru(III) compounds (table 4.9).

Worth mentioning is that these three Ru(III) compounds present quite similar IC₅₀ values in the different cell lines, which suggests that they must share the same structure activity relationships.

A slightly higher cytotoxic effect, for RuL1 and RuL2, has been noticed in the cell lines EVSA-T, IGROV and M19; this may suggest a tissue-selectivity cytotoxic activity.

It is also important to stress that these compounds retain their cytotoxic activity in both hormone-independent (ER-negative, EVSA-T) and hormone-dependent (ER-positive, MFC-7) breast tumour cell lines. There is not satisfactory treatment for hormone-dependent breast tumours, even though they account for about one-third of breast cancer cases [120]. The lack of selectivity for these family of Ru(III) compounds could be beneficial so further studies are needed.

The previous results reveal that the ligand must play a crucial role in tuning the biological activity of the related Ru(III) compounds. In contrary to the conclusions observed for the free ligands, it appears that bulky ligands increase the biological activity upon coordination.

The small structural difference between RuL2 and RuL1, where, RuL2 posses a more bulky ligand, is enough for the 3-fold increase in the cytotoxic activity.

Although a discussion about the mechanism of activity is still premature, it is clear, that the biological activity is affected by both electronic and steric factors. It can be proposed that the steric effects can reduce the rate of hydrolysis or other substitution reactions in the Ru(III) compound and, at the same time, the ligand, a bis(arylimino)pyridine derivative, with the imino moieties (known to have better π -backbonding properties than pyridine) can stabilize more efficiently lower oxidation states of the metal centre. This last effect of the ligand could have a major effect if the proposed "activation by reduction" mechanism would take part in the cells.

Clearly, more studies with different cell lines and *in vitro* studies with biologically relevant structures, like proteins, DNA and reducing agents, and determination of redox properties are required. Also structural modifications that improve the solubility properties will be of help.

Due to the potent cytotoxic results obtained for RuL1 and RuL2, and moreover, the facility of structural modification of the ligand, and as a direct result in the structure of the Ru(III) compounds, the fine tuning of the biological activity constitute the next step in this research project. Then, this family of Ru compounds represents a very promising research option in the field of Ru anticancer compounds.

4.4 Conclusions

The search towards ruthenium complexes with anticancer properties was started in the late nineteen seventies. Due to their low toxicity and good selectivity for metastatic cancer, ruthenium complexes have now become the second option in the design of new metal anticancer drugs. Among several proposals, the "activation by reduction" mechanism has been used to explain the biological activity of some ruthenium derivatives, mainly Ru(III) compounds that, under physiological conditions, are considered kinetically more inert than the corresponding Ru(II) analogues. If this would be the case, the redox properties should be crucial for the biological activity. For the particular case of KP1019 and analogous Ru(III) compounds, it was concluded that differences in the cytotoxic activity correlate with the reduction potentials largely, though not perfectly, which means that other physicochemical properties might be involved.

The peculiar biological behaviour of Ru(III) compounds like NAMI-A, that comprises inactivity towards primary tumours and remarkable activity towards secondary metastasis tumours has stressed the need of more efficient assays for the identification of potential Ru-anticancer compounds apart from the *in vitro* tests. Then the current dominance of the IC_{50} values as a first screen for a putative drug should be treated with caution and moreover, the selection of the appropriate cells targets must become the first task in the study of the Ru-biological activity.

In this chapter, two completely new Ru(III) compounds using versatile tridentate bis(imino)pyridine-type of molecule as chelating ligand, were synthesized in high yields and extensively characterized by standard techniques. The resulting octahedral compounds keep three coordination sites occupied by labile chloride ligands. The interaction of the Ru(III) compounds with the DNA-model base, 9-ethylguanine (9EtGua), was studied and the successful coordination of this model base was demonstrated, both in the solid state and in solution for RuL1, where a peculiar trans conformation was stabilized by intramolecular hydrogen bond interactions.

Remarkable *in vitro* antiproliferative properties for RuL1 and RuL2 were found, as the compounds show potent cytotoxic activity, and up to 6 and 33 times higher activity than the free ligands. In some cell lines the cytotoxic effect of these new Ru(III) compounds proves to be higher than the effect generated by cisplatin and certainly at least one order of magnitude higher than the cytotoxic effect detected for other Ru(III) compounds reported in literature. Even more encouraging results may be expected when structural modifications would improve the solubility properties. Worth mentioning is the fact that RuL2 is the most cytotoxic compound revealing that steric and electronic factors could be determinant in the biological activity. It is evident that more research is needed to establish further structure activity relationships.

Chapter 4

This research has led the development of a promising new generation of potential antineoplastic Ru(III) and Ru(II) compounds with bis(arylimino)pyridine ligands. The potential interest lies mainly in the facility of modifications of the ligand moiety, which could help in the tuning of the biological properties, but also represent plausible active catalytic compounds in the field of metal-bis(imino)pyridine systems that have attracted significant attention in recent years.

The potent cytotoxic activity observed for these family of bis(arylimino)pyridine-Ru(III) compounds stresses the need for more studies comprising the *in vitro* cytotoxic activity determination in different cell lines, the interaction with biologically relevant structures, like proteins, DNA, nucleotides and reducing agents (ascorbic acid, cysteine or glutathione), and the redox and aquation/hydrolysis properties as well. Also structural modifications that improve the solubility properties are recommended.

These new Ru(III) compounds also represent useful starting materials for the synthesis of other mononuclear Ru(II) species by replacement of the chloride ligands under appropriate experimental conditions. The following chapter comprises the exploration of such possibilities and the search of structure activity relationships.

4.5 References

- [1] B. Rosenberg, L. Vancamp, T. Krigas, *Nature* 205 (1965) 698.
- [2] M.J. Clarke, F.C. Zhu, D.R. Frasca, *Chem. Rev.* 99 (1999) 2511-2533.
- [3] M.J. Cleare, *Coord. Chem. Rev.* 12 (1974) 349-405.
- [4] P. Köpf-Maier, *Eur. J. Clin. Pharmacol.* 47 (1994) 1-16.
- [5] P. Köpf-Maier, H. Kopf, *Chem. Rev.* 87 (1987) 1137-1152.
- [6] I. Ott, R. Gust, *Arch. Pharm.* 340 (2007) 117-126.
- [7] P.J. Sadler, *Adv. Inorg. Chem.* 36 (1991) 1-48.
- [8] C.S. Allardyce, P.J. Dyson, *Platinum Metals Rev.* 45 (2001) 62-69.
- [9] W.H. Ang, P.J. Dyson, *Eur. J. Inorg. Chem.* (2006) 4003-4018.
- [10] M.J. Clarke, *Coord. Chem. Rev.* 236 (2003) 209-233.
- [11] A.C.G. Hotze, M. Bacac, A.H. Velders, B.A.J. Jansen, H. Kooijman, A.L. Spek, J.G. Haasnoot, J. Reedijk, *J. Med. Chem.* 46 (2003) 1743-1750.
- [12] A.C.G. Hotze, A.H. Velders, F. Ugozzoli, M. Biagini-Cingi, A.M. Manotti-Lanfredi, J.G. Haasnoot, J. Reedijk, *Inorg. Chem.* 39 (2000) 3838-3844.
- [13] L. Ronconi, P.J. Sadler, *Coord. Chem. Rev.* 251 (2007) 1633-1648.
- [14] Y.K. Yan, M. Melchart, A. Habtemariam, P.J. Sadler, *Chem. Commun.* (2005) 4764-4776.
- [15] C.X. Zhang, S.J. Lippard, *Curr. Opin. Chem. Biol.* 7 (2003) 481-489.
- [16] C.G. Hartinger, S. Zorbas-Seifried, M.A. Jakupec, B. Kynast, H. Zorbas, B.K. Keppler, *J. Inorg. Biochem.* 100 (2006) 891-904.
- [17] I. Kostova, *Curr. Med. Chem.* 13 (2006) 1085-1107.
- [18] J.M. Rademaker-Lakhai, D. van den Bongard, D. Pluim, J.H. Beijnen, J.H.M. Schellens, *Clin. Cancer Res.* 10 (2004) 3717-3727.
- [19] J. Reedijk, *Platinum Metals Rev.* 52 (2008) 2-11.
- [20] J.K. Barton, *Science* 233 (1986) 727-734.
- [21] J.K. Barton, E. Lolis, *J. Am. Chem. Soc.* 107 (1985) 708-709.
- [22] V. Brabec, O. Novakova, *Drug Resist. Update* 9 (2006) 111-122.
- [23] P.J. Dandliker, R.E. Holmlin, J.K. Barton, *Science* 275 (1997) 1465-1468.
- [24] K.E. Erkkila, D.T. Odom, J.K. Barton, *Chem. Rev.* 99 (1999) 2777-2795.
- [25] A. Greguric, I.D. Greguric, T.W. Hambley, J.R. Aldrich-Wright, J.G. Collins, *J. Chem. Soc.-Dalton Trans.* (2002) 849-855.
- [26] N. Grover, T.W. Welch, T.A. Fairley, M. Cory, H.H. Thorp, *Inorg. Chem.* 33 (1994) 3544-3548.
- [27] C.W. Jiang, H. Chao, X.L. Hong, H. Li, W.J. Mei, L.N. Ji, *Inorg. Chem. Commun.* 6 (2003) 773-775.
- [28] C.W. Jiang, H. Chao, H. Li, L.N. Ji, *J. Inorg. Biochem.* 93 (2003) 247-255.
- [29] C.W. Jiang, H. Chao, R.H. Li, H. Li, L.N. Jia, *J. Coord. Chem.* 56 (2003) 147-154.
- [30] R.C. Lasey, S.S. Banerji, M.Y. Ogawa, *Inorg. Chim. Acta* 300 (2000) 822-828.
- [31] J.G. Liu, B.H. Ye, Q.L. Zhang, X.H. Zou, Q.X. Zhen, X. Tian, L.N. Ji, *J. Biol. Inorg. Chem.* 5 (2000) 119-128.
- [32] J.G. Liu, Q.L. Zhang, X.F. Shi, L.N. Ji, *Inorg. Chem.* 40 (2001) 5045-5050.
- [33] G.A. Neyhart, C.C. Cheng, H.H. Thorp, *J. Am. Chem. Soc.* 117 (1995) 1463-1471.
- [34] A.M. Pyle, J.K. Barton, *Prog. Inorganic Chem.* 38 (1990) 413-475.
- [35] A.M. Pyle, J.P. Rehmann, R. Meshoyrer, C.V. Kumar, N.J. Turro, J.K. Barton, *J. Am. Chem. Soc.* 111 (1989) 3051-3058.
- [36] Y. Xiong, X.F. He, X.H. Zou, J.Z. Wu, X.M. Chen, L.N. Ji, R.H. Li, J.Y. Zhou, K.B. Yu, *J. Chem. Soc.-Dalton Trans.* (1999) 19-23.
- [37] Q.X. Zhen, B.H. Ye, Q.L. Zhang, J.G. Liu, H. Li, L.N. Ji, L. Wang, *J. Inorg. Biochem.* 76 (1999) 47-53.
- [38] O. Novakova, J. Kasparkova, O. Vrana, P.M. van Vliet, J. Reedijk, V. Brabec, *Biochemistry* 34 (1995) 12369-12378.

Chapter 4

- [39] P.M. van Vliet, S.M.S. Toekimin, J.G. Haasnoot, J. Reedijk, O. Novakova, O. Vrana, V. Brabec, *Inorg. Chim. Acta* 231 (1995) 57-64.
- [40] R. Balamurugan, M. Palaniandavar, M.A. Halcrow, *Polyhedron* 25 (2006) 1077-1088.
- [41] S.C. Bart, E. Lobkovsky, E. Bill, K. Wieghardt, P.J. Chirik, *Inorg. Chem.* 46 (2007) 7055-7063.
- [42] C. Bianchini, G. Giambastiani, I.G. Rios, G. Mantovani, A. Meli, A.M. Segarra, *Coord. Chem. Rev.* 250 (2006) 1391-1418.
- [43] G.J.P. Britovsek, V.C. Gibson, O.D. Hoarau, S.K. Spitzmesser, A.J.P. White, D.J. Williams, *Inorg. Chem.* 42 (2003) 3454-3465.
- [44] B. de Bruin, E. Bill, E. Bothe, T. Weyhermuller, K. Wieghardt, *Inorg. Chem.* 39 (2000) 2936-2947.
- [45] V.C. Gibson, C. Redshaw, G.A. Solan, *Chem. Rev.* 107 (2007) 1745-1776.
- [46] G.G. Mohamed, *Spectroc. Acta Pt. A-Molec. Biomolec. Spectr.* 64 (2006) 188-195.
- [47] S. McTavish, G.J.P. Britovsek, T.M. Smit, V.C. Gibson, A.J.P. White, D.J. Williams, *J. Mol. Catal. A-Chem.* 261 (2007) 293-300.
- [48] R.C. Stoufer, D.H. Busch, *J. Am. Chem. Soc.* 78 (1956) 6016-6019.
- [49] F. Lions, K.V. Martin, *J. Am. Chem. Soc.* 79 (1957) 2733-2738.
- [50] G.J.P. Britovsek, V.C. Gibson, B.S. Kimberley, P.J. Maddox, S.J. McTavish, G.A. Solan, A.J.P. White, D.J. Williams, *Chem. Commun.* (1998) 849-850.
- [51] G.J.P. Britovsek, V.C. Gibson, B.S. Kimberley, S. Mastroianni, C. Redshaw, G.A. Solan, A.J.P. White, D.J. Williams, *J. Chem. Soc.-Dalton Trans.* (2001) 1639-1644.
- [52] B.L. Small, M. Brookhart, *J. Am. Chem. Soc.* 120 (1998) 7143-7144.
- [53] B.L. Small, M. Brookhart, A.M.A. Bennett, *J. Am. Chem. Soc.* 120 (1998) 4049-4050.
- [54] D. Enright, S. Gambarotta, G.P.A. Yap, P.H.M. Budzelaar, *Angew. Chem.-Int. Edit.* 41 (2002) 3873-3876.
- [55] Nonius, COLLECT; Nonius BV, Delft: The Netherlands (1999).
- [56] A.M.M. Schreurs, PEAKREF, University of Utrecht: The Netherlands (2005).
- [57] A.J.M. Duisenberg, L.M.J. Kroon-Batenburg, A.M.M. Schreurs, *J. Appl. Cryst.* 36 (2003) 220-229.
- [58] G.M. Sheldrick, SHELXS86; University of Göttingen: Germany (1986).
- [59] P.T. Beurskens, G. Beurskens, R. de Gelder, S. Garcia-Granda, R.O. Gould, R. Israel, J.M.M. Smits, The DIRDIF99 Program System, Technical Report of the Crystallography Laboratory; University of Nijmegen: The Netherlands (1999).
- [60] G.M. Sheldrick, *Acta Cryst. A* 64 (2008) 112-122.
- [61] G.M. Sheldrick, SADABS; University of Göttingen: Germany (1999-2003).
- [62] A.L. Spek, *J. Appl. Crystallogr.* 36 (2003) 7-13.
- [63] Y.P. Keepers, P.E. Pizao, G.J. Peters, J. Vanarkotte, B. Winograd, H.M. Pinedo, *Eur. J. Cancer* 27 (1991) 897-900.
- [64] M.R. Boyd, in 'Status of the NCI preclinical antitumour drug discovery screen', ed. NCI, Principles and practice of oncology, 1989, 1-12.
- [65] E.P. Papadopolous, A. Jarrar, C.H. Issidorides, *J. Org. Chem.* 31 (1966) 615-618.
- [66] A.L. Vance, N.W. Alcock, D.H. Busch, J.A. Heppert, *Inorg. Chem.* 36 (1997) 5132-5134.
- [67] G.J.P. Britovsek, M. Bruce, V.C. Gibson, B.S. Kimberley, P.J. Maddox, S. Mastroianni, S.J. McTavish, C. Redshaw, G.A. Solan, S. Stromberg, A.J.P. White, D.J. Williams, *J. Am. Chem. Soc.* 121 (1999) 8728-8740.
- [68] Y.F. Chen, C.T. Qian, J. Sun, *Organometallics* 22 (2003) 1231-1236.
- [69] C. Bianchini, G. Giambastiani, I.R. Guerrero, A. Meli, E. Passaglia, T. Gragnoli, *Organometallics* 23 (2004) 6087-6089.
- [70] C. Bianchini, G. Mantovani, A. Meli, F. Migliacci, F. Zanobini, F. Laschi, A. Sommazzi, *Eur. J. Inorg. Chem.* (2003) 1620-1631.
- [71] Z. Ma, W.H. Sun, Z.L. Li, C.X. Shao, Y.L. Hu, X.H. Li, *Polym. Int.* 51 (2002) 994-997.
- [72] D. Reardon, F. Conan, S. Gambarotta, G. Yap, Q.Y. Wang, *J. Am. Chem. Soc.* 121 (1999) 9318-9325.
- [73] A. Citterio, A. Arnoldi, C. Macri, *Chim. Ind.* 60 (1978) 14-15.
- [74] G. Condorelli, I. Fragala, S. Giuffrida, A. Cassol, *Z. Anorg. Allg. Chem.* 412 (1975) 251-257.
- [75] J.A. Faniran, K.S. Patel, J.C. Bailar, *J. Inorg. Nucl. Chem.* 36 (1974) 1547-1551.
- [76] H.H. Freedman, *J. Am. Chem. Soc.* 83 (1961) 2900-2905.
- [77] A. Seminara, S. Giuffrida, A. Musumeci, I. Fragala, *Inorg. Chim. Acta* 95 (1984) 201-205.
- [78] K. Nakamoto, 'Infrared and Raman Spectra of Inorganic and Coordination Compounds', Wiley, 1980.
- [79] J.M. Holland, X.M. Liu, J.P. Zhao, F.E. Mabbs, C.A. Kilner, M. Thornton-Pett, M.A. Halcrow, *J. Chem. Soc.-Dalton Trans.* (2000) 3316-3324.
- [80] Y. Belokon, M. Moscalenko, N. Ikonnikov, L. Yashkina, D. Antonov, E. Vorontsov, V. Rozenberg, *Tetrahedron: Asymmetry* 8 (1997) 3245-3250.
- [81] X.H. Lu, Q.H. Xia, H.J. Zhan, H.X. Yuan, C.P. Ye, K.X. Su, G. Xu, *J. Mol. Catal. A* 205 (2006) 62-69.
- [82] H. Karaer, *Turk. J. Chem* 23 (1999) 67-71.
- [83] E.L. Dias, M. Brookhart, P.S. White, *Organometallics* 19 (2000) 4995-5004.
- [84] B. Cetinkaya, E. Cetinkaya, M. Brookhart, P.S. White, *J. Mol. Catal. A-Chem.* 142 (1999) 101-112.
- [85] G.J.P. Britovsek, J. England, S.K. Spitzmesser, A.J.P. White, D.J. Williams, *Dalton Trans.* (2005) 945-955.
- [86] W.M. Reiff, N.E. Erickson, W.A. Baker, *Inorg. Chem.* 8 (1969) 2019-2021.
- [87] J.P. Sauvage, J.P. Collin, J.C. Chambron, S. Guillerez, C. Coudret, V. Balzani, F. Barigelletti, L. Decola, L. Flamigni, *Chem. Rev.* 94 (1994) 993-1019.
- [88] B. Mondal, S. Chakraborty, P. Munshi, M.G. Walawalkar, G.K. Lahiri, *J. Chem. Soc.-Dalton Trans.* (2000) 2327-2335.
- [89] B. Mondal, H. Paul, V.G. Puranik, G.K. Lahiri, *J. Chem. Soc.-Dalton Trans.* (2001) 481-487.
- [90] B. Mondal, M.G. Walawalkar, G.K. Lahiri, *J. Chem. Soc.-Dalton Trans.* (2000) 4209-4217.

Chapter 4

- [91] A. Gerli, J. Reedijk, M.T. Lakin, A.L. Spek, *Inorg. Chem.* 34 (1995) 1836-1843.
- [92] N.C. Pramanik, K. Pramanik, P. Ghosh, S. Bhattacharya, *Polyhedron* 17 (1998) 1525-1534.
- [93] H. tom Dieck, K.-D. Franz, F. Hohmann, *Chem. Ber.* 108 (1975) 163-173.
- [94] T.D. Thangadurai, S.K. Ihm, *Transit. Met. Chem.* 29 (2004) 189-195.
- [95] J.P. Collman, 'Principles and applications of Organotransition Metal Chemistry', University Science Books, 1987.
- [96] K. Matyjaszewski, B. Gobelt, H.J. Paik, C.P. Horwitz, *Macromolecules* 34 (2001) 430-440.
- [97] E.A. Seddon, K.R. Seddon, 'The Chemistry of Ruthenium', ed. C.R.J. H., Elsevier, 1984.
- [98] C.R. Hecker, A.K.I. Gushurst, D.R. McMillin, *Inorg. Chem.* 30 (1991) 538-541.
- [99] K.J. Takeuchi, M.S. Thompson, D.W. Pipes, T.J. Meyer, *Inorg. Chem.* 23 (1984) 1845-1851.
- [100] M.-a. Haga, T. Takasugi, A. Tomie, M. Ishizuya, T. Yamada, M.D. Hossain, M. Inoue, *Dalton Trans.* (2003) 2069-2079.
- [101] K. van der Schilden, 'Polynuclear Ruthenium and Platinum Polypyridyl Complexes', PhD Thesis, Leiden University, Leiden, 2006.
- [102] A.H. Velders, B. van der Geest, H. Kooijman, A.L. Spek, J.G. Haasnoot, J. Reedijk, *Eur. J. Inorg. Chem.* (2001) 369-372.
- [103] P.J. Dyson, G. Sava, *Dalton Trans.* (2006) 1929-1933.
- [104] D. Pluim, R. van Waardenburg, J.H. Beijnen, J.H.M. Schellens, *Cancer Chemother. Pharmacol.* 54 (2004) 71-78.
- [105] G. Sava, I. Capozzi, A. Bergamo, R. Gagliardi, M. Cocchietto, L. Masiero, M. Onisto, E. Alessio, G. Mestroni, S. Garbisa, *Int. J. Cancer* 68 (1996) 60-66.
- [106] G. Sava, S. Pacor, A. Bergamo, M. Cocchietto, G. Mestroni, E. Alessio, *Chem.-Biol. Interact.* 95 (1995) 109-126.
- [107] V.J. Catalano, R.A. Heck, A. Ohman, M.G. Hill, *Polyhedron* 19 (2000) 1049-1055.
- [108] V.J. Catalano, R.A. Heck, C.E. Immoos, A. Ohman, M.G. Hill, *Inorg. Chem.* 37 (1998) 2150-2157.
- [109] F. Zobi, M. Hohl, W. Zimmermann, R. Alberto, *Inorg. Chem.* 43 (2004) 2771-2772.
- [110] M. Ravera, S. Baracco, C. Cassino, D. Colangelo, G. Bagni, G. Sava, D. Osella, *J. Inorg. Biochem.* 98 (2004) 984-990.
- [111] M. Ravera, C. Cassino, S. Baracco, D. Osella, *Eur. J. Inorg. Chem.* (2006) 740-746.
- [112] M.J. Clarke, *Coord. Chem. Rev.* 236 (2002) 209-233.
- [113] G. Sava, F. Frausin, M. Cocchietto, F. Vita, E. Podda, P. Spessotto, A. Furlani, V. Scarcia, G. Zabucchi, *Eur. J. Cancer* 40 (2004) 1383-1396.
- [114] E. Reisner, V.B. Arion, B.K. Keppler, A.J.L. Pombeiro, *Inorg. Chim. Acta* 361 (2008) 1569-1583.
- [115] M.A. Jakupec, E. Reisner, A. Eichinger, M. Pongratz, V.B. Arion, M. Galanski, C.G. Hartinger, B.K. Keppler, *J. Med. Chem.* 48 (2005) 2831-2837.
- [116] M. Groessl, E. Reisner, C.G. Hartinger, R. Eichinger, O. Semenova, A.R. Timerbaev, M.A. Jakupec, V.B. Arion, B.K. Keppler, *J. Med. Chem.* 50 (2007) 2185-2193.
- [117] V.B. Arion, E. Reisner, M. Fremuth, M.A. Jakupec, B.K. Keppler, V.Y. Kukushkin, A.J.L. Pombeiro, *Inorg. Chem.* 42 (2003) 6024-6031.
- [118] C.S.R. Menezes, L. Costa, V.D. Avila, M.J. Ferreira, C.U. Vieira, L.A. Pavanin, M.I. Homs-Brandeburgo, A. Hamaguchi, E.D. Silveira-Lacerda, *Chem.-Biol. Interact.* 167 (2007) 116-124.
- [119] S.R. Grguric-Sipka, R.A. Vilaplana, J.M. Perez, M.A. Fuertes, C. Alonso, Y. Alvarez, T.J. Sabo, F. Gonzalez-Vilchez, *J. Inorg. Biochem.* 97 (2003) 215-220.
- [120] P. Pigeon, S. Top, A. Vessieres, M. Hucho, E.A. Hillard, E. Salomon, J. G., *J. Med. Chem.* 48 (2005) 2814-2821.